Formation of Divacancies During Quenching and Annealing in Body-Centered-Cubic Metals*

MASAO DOYAMA
Argonne National Laboratory, Argonne, Illinois
(Received 13 February 1967)

Divacancies and trivacancies in body-centered-cubic metals are classified and discussed for the nearest-neighbor and the next-nearest-neighbor interaction. The general kinetic equations are given. The formation of divancancies during quenching and annealing is discussed in detail.

I. INTRODUCTION

VACANCIES play an important role in the motion of atoms in face-centered cubic metals. Huntington and Seitz[1] first proposed that the self-diffusion in fcc metals is conducted by a vacancy mechanism. This mechanism is verified by quenching experiments.[2] In recent years experimental techniques[3–5] have been developed to quench the metals which oxidize upon heating in air. Schultz[4] quenched tungsten in liquid-helium II and has shown that the self-diffusion in tungsten, a body-centered cubic metal, is probably also conducted by a vacancy mechanism. He found that the formation energy of a vacancy in tungsten to be 3.30 eV. He also cold-worked tungsten and obtained the activation energy in Stage III to be 1.70–1.95 eV.[4] The activation energy for the self-diffusion in tungsten is reported to be 5.23 eV.[6] He obtained the activation energy for the motion of a vacancy in tungsten to be 1.93 eV assuming that the self-diffusion is conducted by a vacancy mechanism. Recently Galligan measured the activation energy for the motion of a vacancy in tungsten using a field ion microscope and determined the activation energy for the motion of a vacancy to be 2.0 eV in tungsten.[7] In a fcc metal, most of the point defects present at high temperatures are vacancies because the energy to form an interstitial is rather high. In bcc metals on the other hand, the energy to form an interstitial is probably not as high as in fcc metals because the bcc lattice is not as closely packed and has more vacant space. It is, however, clear that vacancies play an important role for the motion of atoms in bcc metals.

Divacancies in fcc metals are commonly observed and are always more mobile than single vacancies in fcc metals. Seitz[8] first suggested that there may exist a positive attractive binding energy between two vacancies. Bartlett and Dienes[9] estimated that the binding energy of a divacancy is between 0.23 and 0.59 eV in copper. The binding energy of divacancies in certain metals is summarized in Table I.[9–22]

When a metal is quenched from a high temperature, divacancies are formed during quenching even in a high-speed quench. The formation and breakup of divacancies during the quench was first treated analytically by Koehler, Seitz, and Bauerle.[23] There exists a critical temperature T^* above which single vacancies and divacancies are still in thermal equilibrium with each other. Below T^* the single vacancies do not move fast enough to maintain the thermal equilibrium between single vacancies and divacancies. Fujiwara[24] calculated the formation of divacancies during a quench using a digital computer. Cotterill[25] used an analog computer and plotted these reactions. Mori, Meshii, and Kauff-

* Based on work performed under the auspices of the U. S. Atomic Energy Commission.

[1] H. B. Huntington and F. Seitz, Phys. Rev. **61**, 315 (1942); H. B. Huntington, *ibid.* **61**, 325 (1942).

[2] For example, J. E. Bauerle and J. S. Koehler, Phys. Rev. **107**, 1493 (1957).

[3] M. Doyama and J. S. Koehler, Phys. Rev. **119**, 939 (1960); **127**, 21 (1962).

[4] H. Schultz, in *Lattice Defects in Quenched Metals*, edited by R. M. J. Cotterill, M. Doyama, J. J. Jackson, and M. Meshii (Academic Press Inc., New York, 1965), p. 761; Acta Met. **12**, 649 (1964).

[5] M. H. Loretto, L. M. Clarebrough, and R. L. Segall, International Conference on Electron Diffraction and Crystal Defects, Melbourne, 1965, II G-3 (unpublished).

[6] W. Danneberg, Metall. **15**, 977 (1961).

[7] J. Galligan (private communication).

[8] F. Seitz, Advan. Phys. **1**, 43 (1952).

[9] S. H. Bartlett and G. J. Dienes, Phys. Rev. **89**, 848 (1953).

[10] T. Mori, M. Meshii, and J. W. Kauffman, J. Appl. Phys. **33**, 2776 (1962).

[11] J. W. Kauffman and M. Meshii, in *Lattice Defects in Quenched Metals*, edited by R. M. J. Cotterill, M. Doyama, J. J. Jackson, and M. Meshii (Academic Press Inc., New York, 1965), p. 77.

[12] J. A. Ytterhus, R. W. Siegel, and R. W. Balluffi, in *Lattice Defects in Quenched Metals*, edited by R. M. J. Cotterill, M. Doyama, J. J. Jackson, and M. Meshii (Academic Press Inc., New York, 1965), p. 679.

[13] R. W. Balluffi and R. W. Siegel, in *Lattice Defects in Quenched Metals*, edited by R. M. J. Cotterill, M. Doyama, J. J. Jackson, and M. Meshii (Academic Press Inc., New York, 1965), p. 593.

[14] M. de Jong and J. S. Koehler, Phys. Rev. **129**, 40 (1963); *ibid.* **129**, 49 (1963).

[15] T. Kino and J. S. Koehler, Bull. Am. Phys. Soc. **11**, 183 (1966).

[16] A. Seeger, Phys. Letters **9**, 311 (1964).

[17] M. Doyama and J. S. Koehler, Phys. Rev. **134**, A522 (1964).

[18] V. G. Weizer and L. A. Girifalco, Phys. Rev. **120**, 837 (1960).

[19] M. Doyama and R. M. J. Cotterill, in *Lattice Defects and their Interactions*, edited by R. R. Hasiguti (Gordon and Breach Publishers, New York, 1967).

[20] A. Seeger, J. Phys. Radium **23**, 616 (1962).

[21] A. Seeger and H. Bross, Z. Physik **145**, 161 (1956); J. Phys. Chem. Solids **16**, 253 (1960).

[22] R. A. Johnson, Phys. Rev. **134**, A1329 (1964).

[23] J. S. Koehler, F. Seitz, and J. E. Bauerle, Phys. Rev. **107**, 1499 (1957).

[24] H. Fujiwara, Technical Report of the University of Illinois, 1960 (unpublished).

[25] R. M. J. Cotterill, in *Lattice Defects in Quenched Metals*, edited by R. M. J. Cotterill, M. Doyama, J. J. Jackson, and M. Meshii (Academic Press Inc., New York, 1965), p. 97.

TABLE I. Binding energy of a divacancy.

Metal		eV	References
Au	0.1	(E)[a]	2, 14
	0.1∼0.2	(E)	15
	0.3	(E)	10, 11
			12, 13
Ag	0.38	(E)	3
	0.19	(E)	16
Al	0.17	(E)	17
Cu	0.23–0.59	(T)	9
	0.64	(T)	18
	0		19
	0.1∼0.2	(T)	20, 21
Fe	0.20	(T)	22

[a] (E) means an experimental and T a theoretical value.

man[10] carried out systematic experiments to study the effect of the quenching rate on quenched-in vacancies. This work was carefully reexamined by Flynn, Bass, and Lazarus.[26] Kimura, Maddin, and Kuhlmann-Wilsdorf[27] also examined the process. Koehler, de Jong, and Seitz[28] calculated the critical temperature T^* for a linear and exponential quench. Doyama[29] extended this treatment to a general quenching. Much work remains to be done in this important field of vacancies and vacancy clusters in bcc metals. In this paper the formation of divacancies in bcc metals during quenching and annealing is discussed in detail.

II. SINGLE VACANCIES IN BODY-CENTERED-CUBIC METALS

In Fig. 1(a) site A represents a single vacancy in a body-centered cubic metal. When atom B moves to vacant site A, atom B has to squeeze through the hole at N, the center of triangle CDE and M, the center of triangle FGH. There are two peaks in the energy of the system when atom B moves to site A [Fig. 1(b)]. Activation energy for the motion of a single vacancy is represented by E^M in Fig. 1(b). At I, which is the middle point of sites A and B, the energy of the crystal has a local minimum. There are two half vacancies at sites A and B and an interstitial atom at I for this configuration. This configuration will be called "activated single vacancy." This configuration is metastable. Let the energy at I be E_1' higher than the energy at a position where the vacancy is stable. Let the fractional concentrations of single vacancies and activated single vacancies be C_1 and C_I. At thermal equilibrium the following relation is obtained.

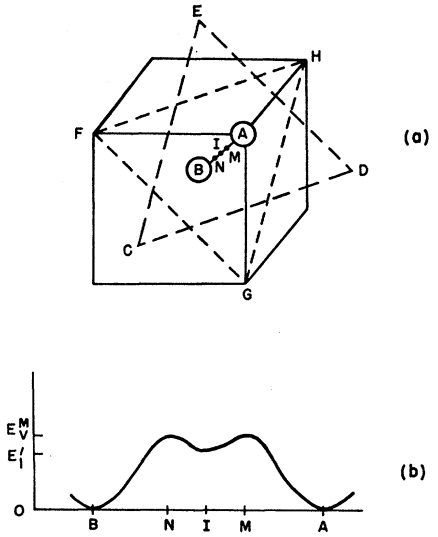

FIG. 1. (a) Site A represents a single vacancy in a body-centered cubic metal. When atom A moves to vacant site A, atom B squeezes through the hole at N, the center of triangle CDE and M, the center of triangle GFH. (b) Schematic diagram for the motion of vacancy in a body-centered metal. There are two peaks in the energy of the system. At I, which is the middle point of sites A and B, the system has metastable state.

$$C_I/C_1 = A \exp(-E_1'/kT), \tag{1}$$

where A is a constant.

III. DIVACANCIES IN BODY-CENTERED CUBIC-METALS

A divacancy in a face-centered cubic metal is shown in Fig. 2(a). It has four common nearest-neighbor atoms to two vacant sites and fourteen nearest-neighbor atoms to one vacant site. In a body-centered cubic metal, the type-I divacancy has no common nearest-neighbor atoms to two vacant sites but all fourteen nearest-neighbor atoms are at least one nearest neighbor to one vacant site. The type-II divacancy shown in Fig. 2 has two vacant sites in the next-nearest neighbor-positions. This configuration has four common neighbors. Let the radius of an atom in a bcc metal be r_0, which is half of the nearest-neighbor distance. For the motion of a single vacancy, dotted lines in Fig. 3(a) show the planes of two saddle points ({111} planes) as described in Sec. II. At the saddle points the radius of the hole for the motion of a single vacancy in a hard-sphere model is $(4\sqrt{2}/3-1)r_0=0.885r_0$. For the motion of type-I divacancies, the divacancy has to be broken up into (1) type-II divacancy or (2) two isolated vacancies which are more than next-neighbor distance apart. The motion from type I to type II is shown in Fig. 3(a). One

[26] C. P. Flynn, J. Bass, and D. Lazarus, in *Lattice Defects in Quenched Metals*, edited by R. M. J. Cotterill, M. Doyama, J. J. Jackson, and M. Meshii (Academic Press Inc., New York, 1965), p. 639.

[27] H. Kimura, R. Maddin, and D. Kuhlmann-Wilsdorf, Acta Met. 7, 154 (1959).

[28] J. S. Koehler, M. de Jong, and F. Seitz, Proceedings of the International Conference on Crystal Lattice Defects, 1962 (unpublished); J. Phys. Soc. Japan 18, Suppl. 3, 1 (1963).

[29] M. Doyama, in *Lattice Defects in Quenched Metals*, edited by R. M. J. Cotterill, M. Doyama, J. J. Jackson, and M. Meshii (Academic Press Inc. New York, 1965), p. 167

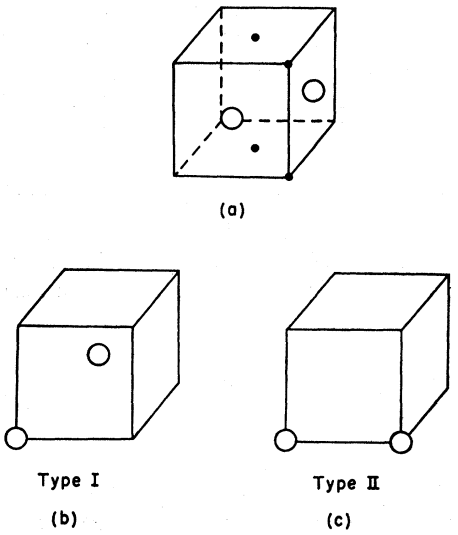

FIG. 2. Divacancies. (a) a divacancy in a face-centered cubic metal. Four black points are the positions of the four common nearest-neighbor atoms for the divacancy. (b) Type-I divacancy in a body-centered cubic metal. Two vacant sites are nearest neighbor each other. (c) Type-II divacancy in a body-centered cubic metal. Two vacant sites are next-nearest neighbor.

of the locking atoms on one of the two saddle-point planes is missing. Atom A can squeeze through this triangle with less activation energy than is required for the motion of a single vacancy. Atom A, however, has to go through the center of the other triangle. The activation energy for this process is then almost the same as that of the motion of a single vacancy. Also, for the motion of a divacancy, the additional energy difference, $B_{2I}-B_{2II}$, between the binding energy of type I (B_{2I}) and type II (B_{2II}) is required.

The motion of type II to type I is the reverse of the process discussed above. In this case the motion of a type-II divacancy is also as easy as the motion of a single vacancy. A divacancy can move through type I and type II in an alternating manner.

Eight nearest-neighbor bonds are broken to form a vacancy in a bcc metal. One of the eight atoms next to the vacancy has to be removed to make a type-I divacancy. Seven bonds are broken for this process. In a very simple and naïve calculation, the binding energy of a divacancy in a bcc metal is about one-eighth of the nearest-neighbor bond. If the electron redistribution and extra relaxation around a divacancy are neglected, the binding energy of a divacancy in a bcc metal is about one-fourth of the formation energy of a single vacancy. The binding energy of a type-II divacancy is probably not much different from a type-I divacancy because the distances between two vacant sites are d_0 and $2d_0/\sqrt{3}$ for type I and type II, respectively. The values of the pairwise potential for these two cases are not very different.[22,30–32]

Johnson[22] calculated the binding energy and the activation energy for the migration of a divacancy in iron using a pairwise interaction. He obtained the binding energies of type-I and type-II divacancies in iron to be 0.13 and 0.2 eV, respectively. He also calculated the activation energy for the motion of a vacancy in iron and obtained 0.68 eV. For the migration of a divacancy from type II to type I he obtained 0.66 eV. This calculation is consistent with the explanation given in the preceding paragraph.

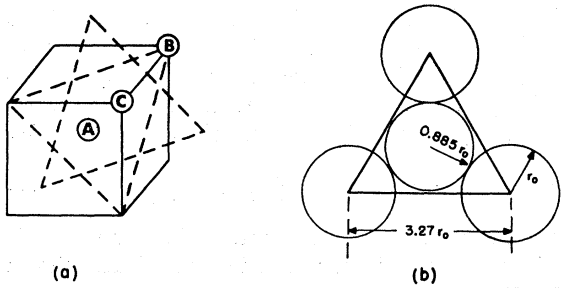

FIG. 3. (a) Motion of divacancy type I. Two vacant sites are at A and B. Type I can be changed to type II which vacant sites are at A and C by squeezing atom C to site A. (b) Triangle at the saddle point for the motion of a vacancy in a body-centered cubic metal. For the motion of a divacancy one of the atoms on one triangle is missing.

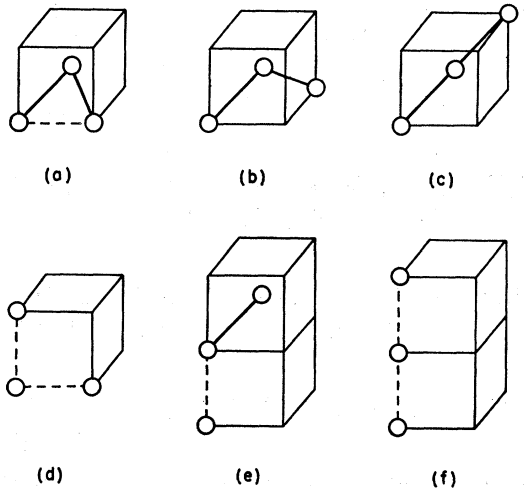

FIG. 4. Configurations of trivacancies in a body-centered metal. Solid thick lines represent nearest-neighbor bonds and dotted lines represent next-nearest-neighbor bonds. (a) 71° trivacancy, (b) 109° trivacancy, (c) 180°(I) trivacancy, (d) 90° trivacancy, (e) 144° trivacancy, and (f) 180°(II) trivacancy.

IV. TRIVACANCIES IN BODY-CENTERED CUBIC-METALS

Trivacancies in a face-centered cubic lattice have four configurations.[14,28] de Jong and Koehler classified these

[30] R. M. J. Cotterill and M. Doyama, Bull. Am. Phys. Soc. **11**, 219 (1966).
[31] M. Doyama and R. M. J. Cotterill, Bull. Am. Phys. Soc. **11**, 460 (1966).
[32] L. A. Girifalco and V. G. Weizer, Phys. Rev. **114**, 687 (1959).

configurations and named them "doglegs." In a body-centered cubic lattice there are three configurations and these are shown in (a), (b), and (c) in Fig. 4. The angles between the nearest neighbor bonds are 70° 32′, 109° 28′, and 180°. These will hereafter be called 71° trivacancy, 109° trivacancy, and 180°(I) trivacancy, respectively. When the next-nearest-neighbor bonds are considered, there are three more configurations which are shown in (d), (e), and (f) in Fig. 4. The angles between the bonds are 90°, 144°, and 180°. These will hereafter be called 90° trivacancy, 144° trivacancy, and 180°(II) trivacancy, respectively. In Fig. 4 the nearest-neighbor bonds are shown with solid lines and the next-nearest-neighbor bonds are shown with broken lines. In a fcc metal the common nearest neighbor of a 60° trivacancy relaxes to the center of the tetrahedron formed by the common nearest neighbor and three vacancies.[33,34] A similar large relaxation, however, does not occur in the trivacancies in a bcc metal. The trivacancies are probably as mobile as the divacancies in a bcc metal.

V. NEAREST-NEIGHBOR INTERACTION

In this section the interaction between atoms farther than the nearest-neighbor interaction is ignored, and only the nearest-neighbor interaction is considered.

A. General Kinetic Equations

The phenomenological kinetic equations for pure metals assuming the nearest-neighbor interactions are:

$$dC_1/dt=-2\alpha(VV\rightarrow d;A)C_1^2+2\alpha(d\rightarrow V,V;A)C_2-\alpha(d,V\rightarrow t^{71};A_2)C_1C_2+\alpha(t^{71}\rightarrow d,V;A)C_3^{71}$$
$$-\alpha(d,V\rightarrow t^{109};A)C_1C_2+\alpha(t^{109}\rightarrow d,V;A)C_3^{109}-\alpha(d,V\rightarrow t^{180};A)C_1C_2+\alpha(t^{180}\rightarrow d,V;A)C_3^{180}$$
$$-\alpha(V,V,V\rightarrow t^{71};A_2)C_1^3+3\alpha(t^{71}\rightarrow V,V,V;A)C_3^{71}-\alpha(V,V,V\rightarrow t^{109};A_3)C_1^3$$
$$+3\alpha(t^{109}\rightarrow V,V,V;A)C_3^{109}-\alpha(V,V,V\rightarrow t^{180};A_3)C_1^3+3\alpha(t^{180}\rightarrow V,V,V;A)C_3^{180}$$
$$-\alpha(V,t^{71}\rightarrow te;A)C_1C_3^{71}+D_1\nabla^2C_1; \quad (2a)$$

$$dC_2/dt=+\alpha(V,V\rightarrow d;A)C_1^2-\alpha(d\rightarrow V,V;A)C_2-\alpha(d,V\rightarrow t^{71};A_2)C_1C_2+\alpha(t^{71}\rightarrow d,V;A)C_3^{71}$$
$$-\alpha(d,V\rightarrow t^{109};A)C_1C_2+\alpha(t^{109}\rightarrow d,V;A)C_3^{109}-\alpha(d,V\rightarrow t^{180};A)C_1C_2+\alpha(t^{180}\rightarrow d,V;A)C_3^{180}$$
$$-\alpha(d,d\rightarrow te;A)C_2^2+D_2\nabla^2C_2; \quad (2b)$$

$$dC_3^{71}/dt=+\alpha(d,V\rightarrow t^{71};A_2)C_1C_2-\alpha(t^{71}\rightarrow d,V;A)C_3^{71}-\alpha(t^{71}\rightarrow t^{109};A_2)C_3^{71}+\alpha(t^{109}\rightarrow t^{71};A_2')C_3^{109}$$
$$-\alpha(t^{71}\rightarrow d,V;A)C_3^{71}+\alpha(t,V\rightarrow t^{71};A_2)C_1C_2-\alpha(t^{71}\rightarrow V,V,V;A)C_3^{71}$$
$$+\alpha(V,V,V\rightarrow t^{71};A_2)C_1^3+D_3^{71}\nabla^2C_3^{71}; \quad (2c)$$

$$dC_3^{109}/dt=-\alpha(t^{109}\rightarrow t^{71};A_2')C_3^{109}+\alpha(t^{71}\rightarrow t^{109};A_2)C_3^{71}-\alpha(t^{109}\rightarrow d,V;A)C_3^{109}+\alpha(d,V\rightarrow t^{109};A)C_1C_2$$
$$-\alpha(t^{109}\rightarrow V,V,V;A)C_3^{109}+\alpha(V,V,V\rightarrow t^{109};A_3)C_1^3+D_3^{109}\nabla^2C_3^{109}; \quad (2d)$$

$$dC_3^{180}/dt=-\alpha(t^{180}\rightarrow d,V;A)C_3^{180}+\alpha(d,V\rightarrow t^{180};A)C_1C_2-\alpha(t^{180}\rightarrow V,V,V;A)C_3^{180}$$
$$+\alpha(V,V,V\rightarrow t^{180};A)C_1^3+D_3^{180}\nabla^2C_1^{180}; \quad (2e)$$

$$dC_4/dt=\alpha(t\rightarrow te)C_1C_3+\alpha(d,d\rightarrow te;A)C_2^2+D_4\nabla^2C_4. \quad (2f)$$

In these equations C_1 is the fractional concentration of single vacancies, C_2 is the fractional concentration of divacancies, C_3^{71} is the fractional concentration of 71° trivacancies, C_3^{109} is the fractional concentration of 109° trivacancies, C^{180} is the fractional concentration of 180° trivacancies, and C_4 is the fractional concentration of tetravacancies. (For simplicity only one kind of tetravacancy is included; larger vacancy clusters are excluded.) Rate constants α are given in Table II for the nearest-neighbor interaction. In Fig. 5(a), ν_1 is the frequency of vibration of a shaded atom which is a nearest neighbor of a lattice vacancy. ${}_{71}\nu_2$ is the frequency of vibration of the four shaded atoms [one of which is shown in Fig. 5(b)] which are nearest neighbors to both of the vacancies in a type-II divacancy. ${}_{109}\nu_2$ is the frequency of vibration of the two atoms [Fig. 5(c)] which are nearest neighbors to both of the vacancies which are in the third nearest-neighbor position to each other. ν_3 is the frequency of vibration of the atom [Fig. 5(d)] which has three vacancies. There are a few configurations, one of which is shown in Fig. 5(d). D_1 is the diffusion constant associated with the motion of single vacancies; D_2 is the diffusion constant associated with divacancy migration; D_3 is that associated with trivacancies. E_V^M is the activation energy for the migration of single vacancies, E_d^M is the activation energy associated with the conversion between the 71° trivacancies.

B. Kinetic Equations for the Formation of Divacancies

For the nearest-neighbor interaction the kinetic equations between single vacancies and divacancies in

[33] A. C. Damask, G. J. Dienes, and V. G. Weizer, Phys. Rev. 113, 781 (1959).

[34] R. M. J. Cotterill and M. Doyama, in *Lattice Defects in Quenched Metals*, edited by R. M. J. Cotterill, M. Doyama, J. J. Jackson, and M. Meshii (Academic Press Inc., New York, 1965), p. 653.

TABLE II. The rate constants of the kinetic equations between defects for the nearest-neighbor interaction.

		Reaction	Constants
I	1	$V \rightarrow V$	$\alpha(V \rightarrow V; A) = 8\nu_1 \exp(-E_V{}^M/kT)$
II	1	$d \rightarrow V+V$	$\alpha(d \rightarrow V, V; A) = 14\nu_1 \exp\{-(E_V{}^M+B_2)/kT\}$
III	1	$i^{71} \rightarrow i^{71}$	$\alpha(i^{71} \rightarrow i^{71}; A_2) = 4\ {}_{71}\nu_2 \exp(-E_d{}^M/kT)$
	2	$i^{71} \rightarrow i^{109}$	$\alpha(i^{71} \rightarrow i^{109}; A_2) = 2\ {}_{71}\nu_2 \exp\{-(E_d{}^M+B_i{}^{71}-B_i{}^{109})/kT\}$
	3	$i^{71} \rightarrow d+V$	$\alpha(i^{71} \rightarrow d, V; A) = 10\nu_1 \exp\{-(E_V{}^M+B_i{}^{71}-B_2)/kT\}$
	4	$i^{71} \rightarrow V+V+V$	$\alpha(i^{71} \rightarrow V, V, V; A) = 2\nu_1 \exp\{-(E_V{}^M+B_i{}^{71})/kT\}$
IV	1	$i^{109} \rightarrow i^{71}$	$\alpha(i^{109} \rightarrow i^{71}; A_2) = 2\ {}_{109}\nu_2 \exp\{-(E_d{}^M+B_i{}^{109}-B_i{}^{71})/kT\}$
	2	$i^{109} \rightarrow d+V$	$\alpha(i^{109} \rightarrow d, V; A) = 12\nu_1 \exp\{-(E_V{}^M+B_i{}^{109}-B_2)/kT\}$
	3	$i^{109} \rightarrow V+V+V$	$\alpha(i^{109} \rightarrow V, V, V; A) = 8\nu_1 \exp\{-(E_V{}^M+B_i{}^{109})/kT\}$
V	1	$i^{180} \rightarrow d+V$	$\alpha(i^{180} \rightarrow d, V; A) = 14\nu_1 \exp\{-(E_V{}^M+B_i{}^{180})/kT\}$
		$i^{180} \rightarrow V+V+V$	$\alpha(i^{180} \rightarrow V, V, V; A) = 6\nu_1 \exp\{-(E_V{}^M+B_i{}^{180})/kT\}$
VI	1	$d+V \rightarrow i^{71}$	$\alpha(d, V \rightarrow i^{71}; A) = 24\nu_1 \exp\{-(E_d{}^M+B_2-B_i{}^{71})/kT\}$
	2	$d+V \rightarrow i^{109}$	$\alpha(d, V \rightarrow i^{109}; A) = 24\nu_1 \exp\{-(E_d{}^M+B_2-B_i{}^{109})/kT\}$
	3	$d+V \rightarrow i^{180}$	$\alpha(d, V \rightarrow i^{180}; A) = 14\nu_1 \exp\{-(E_V{}^M+B_2-B_i{}^{180})/kT\}$
VII	1	$V+V+V \rightarrow i^{71}$	$\alpha(V, V, V \rightarrow i^{71}; A_2) = 24\ {}_{71}\nu_2 \exp(-E_d{}^M/kT)$
	2	$V+V+V \rightarrow i^{109}$	$\alpha(V, V, V \rightarrow i^{109}; A_2) = 12\nu_3 \exp(-E_d{}^M/kT)$
	3	$V+V+V \rightarrow i^{180}$	$\alpha(V, V, V \rightarrow i^{180}; A_2) = 6\nu_3 \exp(-E_d{}^M/kT)$
VIII		$V+V \rightarrow d$	$\alpha(V, V \rightarrow d; A) = 56\nu_1 \exp(-E_V{}^M/kT)$

a body-centered-cubic crystal are as follows:

$$\frac{\partial C_1}{\partial t} = -112C_1{}^2\nu_1 \exp\left(-\frac{E_V{}^M}{kT}\right) + 28\nu_2 C_2 \exp\left(-\frac{E_V{}^M+B_2}{kT}\right) - D_1\left\{\frac{\partial^2 C_1}{\partial r^2} + \frac{1}{r}\frac{\partial C_1}{\partial r}\right\}; \quad (3a)$$

$$\frac{\partial C_2}{\partial t} = 56C_1{}^2\nu_1 \exp\left(-\frac{E_V{}^M}{kT}\right) - 14\nu_2 C_2 \exp\left(-\frac{E_V{}^M+B_2}{kT}\right) - D_2\left\{\frac{\partial^2 C_2}{\partial r^2} + \frac{1}{r}\frac{\partial C_2}{\partial r}\right\}, \quad (3b)$$

where C_1 and C_2 are the fractional concentrations of single vacancies and divacancies; ν_1 and ν_2 are the appropriate frequency coefficients for the migration of a vacancy and for the dissociation of a divacancy. D_1 and D_2 are the diffusion constants associated with the motion of single vacancies and divacancies, respectively. $E_V{}^M$ and B_2 are the activation energy for the motion of a single vacancy and the binding energy of a divacancy, respectively. r is the distance from a sink. The geometrical coefficients were derived as follows: a single vacancy has eight nearest neighbors. If another vacancy comes to one of these eight lattice sites, then a divacancy is formed. Each of the eight sites has seven sites from which a vacancy can come in. Each time a divacancy is formed, two single vacancies disappear. The geometrical factor of the first term of Eq. (3a), therefore, is $8\times7\times2=112$. A divacancy has fourteen sites to break up and each breakup forms two single

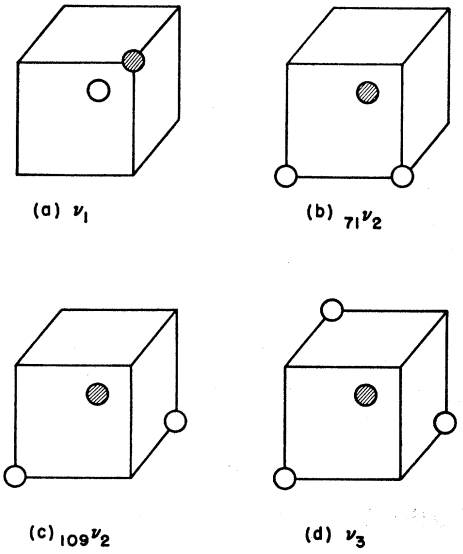

FIG. 5. Definition of vibrating frequencies of atoms next to vacancies in the kinetic equation. (a) ν_1 is the vibrational frequency of an atom next to a vacancy in a bcc metal. (b) ${}_{71}\nu_2$ is the vibrational frequency of an atom common nearest neighbor to a 71° trivacancy. (c) ${}_{109}\nu_2$ is the vibrational frequency of an atom common to a 109° trivacancy. (d) ν_3 is the vibrational frequency of an atom common to three vacancies.

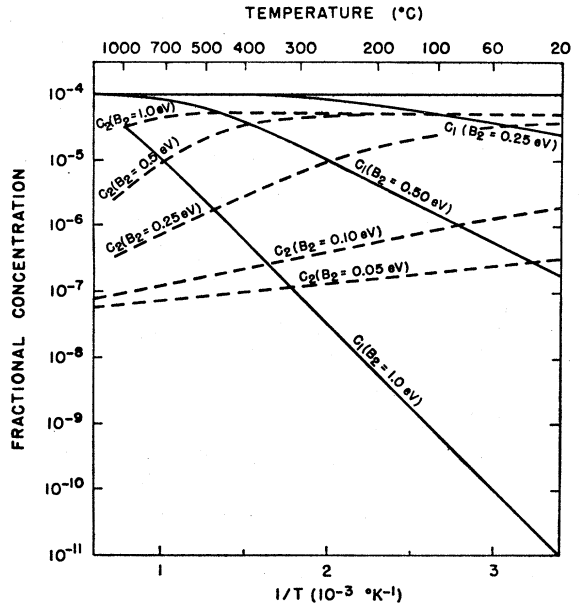

FIG. 6. The equilibrium concentrations of single vacancies and divacancies are plotted with a function of temperature. The total void concentration is 10^{-4}. Figures 6, 7, and 8 are independent of the activation energy for motion or formation energy of a vacancy.

vacancies. The geometrical factor of the second term of Eq. (3a), therefore, is $14\times 2=28$.

C. Thermal Equilibrium

At thermal equilibrium between single vacancies and divacancies the formation and breakup of divacancies are equal, i.e.,

$$C_2=4C_1^2\exp(B_2/kT). \tag{4}$$

When a total void concentration $C_t(=C_1+2C_2)$ is given, C_1 is

$$C_1=\exp(-B_2/kT)\{(1+32C_t\exp(B_2/kT))^{1/2}-1\}/16.$$

The equilibrium concentrations of single vacancies and divacancies are plotted in Figs. 6, 7, and 8 for $C_t=10^{-4}$, 10^{-5}, and 10^{-6}, respectively. These figures are independent of the activation energy for the motion of a vacancy. These figures are good for any body-centered metals. At high temperatures much above T^+ where the fractional concentration of divacancies is much smaller than that of single vacancies, then

$$C_1\simeq C_t.$$

The fractional concentration of divacancies C_2 is

$$C_2=4C_t^2\exp(B_2/kT).$$

When the logarithm of C_t is plotted against $1/T$ at high temperatures C_2 curves show straight lines with the slope of B_2/k. C_1 is constant at high temperatures (Figs. 6, 7, and 8). At low temperatures much below T^+ where the equilibrium fractional divacancy concentration is much higher than that of single vacancies

$$C_2\simeq C_t/2$$

and

$$C_1=(2C_t)^{1/2}\exp(-B_2/2kT)/4.$$

When C_1 is plotted against $1/T$, C_1 curves show straight lines with the slope of $B_2/2k$. C_2 is constant at low temperatures (Figs. 6, 7, and 8). T^+ is given by

$$T^+=-(k/B_2)\ln 4C_1,$$

where T^+ is the temperature at which the fractional concentrations of single vacancies and divacancies are equal.

Koehler, Seitz, and Bauerle[23] and de Jong and Koehler[14] pointed out that a single vacancy will spend a fraction of its life as a single vacancy and the rest of it as a divacancy. In the diffusion process involving lattice vacancies, an effective diffusion constant D, which is given by

$$D=D_1\tau_1/(\tau_1+4\tau_2). \tag{5}$$

The number 4 occurs because the gradients under which single vacancies and divacancies diffuse are coupled by the equilibrium condition. $D_1=\nu_1 a^2\exp(-E_V^M/kT)$ is the diffusion constant for single vacancies. The average life time τ of a single vacancy is given by $1/\tau_1=56\nu_1\times\exp(-E_V^M/kT)$. In pure metal, a single vacancy lives until it encounters another single vacancy forming a divacancy. $1/\tau_2=14\nu_1\exp\{-(E_V^M+B_2)/kT\}$ gives the average lifetime τ_2 of a divacancy which ends when it dissociates into two single vacancies. Assuming that single vacancies and divacancies both diffuse and that

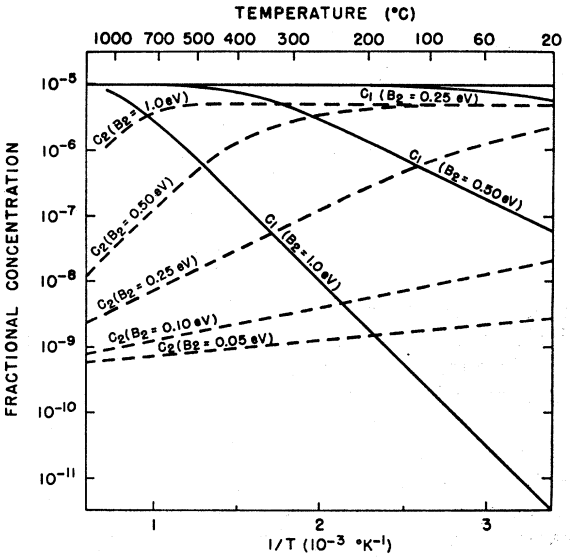

FIG. 7. The equilibrium concentrations of single vacancies and divacancies are plotted with a function of temperature. The total void concentration is 10^{-5}.

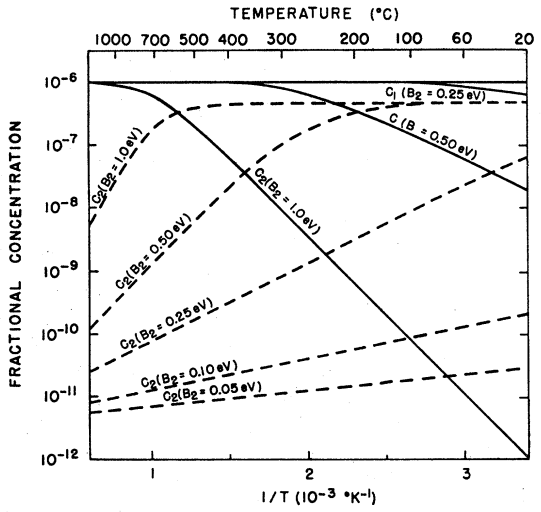

FIG. 8. The equilibrium concentrations of single vacancies and divacancies are plotted against the reciprocal of temperature. The total void concentration is 10^{-6}.

the vacancies and divacancies maintain their local equilibrium ratio, Fick's law requires an appropriate diffusion constant to describe the flow of voids, which in our case is given by D. This can be shown as follows: Let z be the local void concentration, i.e.,

$$z=C_1+2C_2. \tag{6}$$

Assume that a gradient exists in z in the x direction. If the single vacancies and divacancies are in equilibrium with each other, the relative concentration of single vacancies and divacancies is given by Eq. (4). The flux of voids which results from single-vacancy motion can be derived from the gradient of z using (4) and (5).

$$D_1\frac{\partial C_1}{\partial X}=\frac{\nu_1 a^2\exp(-E_V{}^M/kT)}{1+16C_1\exp(B_2/kT)}\frac{dz}{dX}. \tag{7}$$

The total flux of voids J_z is $D_1(\partial C_1/\partial X)$. Fick's law is obeyed, i.e.,

$$J_z=-D(\partial z/\partial X). \tag{8}$$

The effective diffusion constant D is therefore

$$D=\frac{\nu_1 a^2\exp(-E_V{}^M/kT)}{1+16C_1\exp(B_2/kT)}. \tag{9}$$

D. Divacancy Formation During Quenching

Before a specimen is quenched single vacancies and divacancies are in thermal equilibrium at a temperature T_Q, and the temperature of the specimen drops very rapidly during quenching. Divacancies are formed even during a rapid quench. Koehler *et al.*,[23] and Fujiwara[24] show that there exists a critical temperature T^*, above which the reactions between single vacancies and divacancies are still in thermal equilibrium, but below which the single vacancies do not move fast enough to maintain the thermal equilibrium. We assume that no vacancies anneal during quenching. This assumption is not very serious because the annealing of vacancies above T^* does not alter the discussion. The annealing of vacancies only lowers the effective quenching temperature. Then the kinetic equation is

$$\frac{dC_1}{dt}=-112C_1{}^2\nu_1\exp\left(-\frac{E_V{}^M}{kT}\right)+28C_2\nu_1\exp\left(-\frac{E_V{}^M+B_2}{kT}\right). \tag{10}$$

Since it is assumed that no vacancies nor divacancies anneal out from the specimen during quenching, it follows that

$$C_t=\text{const.}=C_1+2C_2. \tag{11}$$

Differentiating Eqs. (4) and (11) with respect to time t the following equations are obtained:

$$\frac{dC_2}{dt}=8C_1\exp\left(\frac{B_2}{kT}\right)\frac{dC_1}{dt}-\frac{4C_1{}^2B_2}{kT}\exp\left(\frac{B_2}{kT}\right)\frac{dT}{dt}, \tag{12}$$

$$\frac{dC_1}{dt}=-2\frac{dC_2}{dt}. \tag{13}$$

Using Eq. (13), Eq. (12) becomes

$$\frac{dT}{dt}=\frac{kT^2}{8B_2C_1{}^2}\exp\left(-\frac{B_2}{kT}\right)\left[1+16C_1\exp\left(\frac{B_2}{kT}\right)\right]\frac{dC_1}{dt}. \tag{14}$$

Here we take the first term of Eq. (12) for the loss of single vacancies, i.e., the formation of divacancies. Then

$$dC_1/dt=-112C_1{}^2\nu_1\exp(-E_V{}^M/kT). \tag{15}$$

From Eqs. (14) and (15), one finds

$$\left(\frac{dT}{dt}\right)=-\frac{14\nu_1kT^2}{B_2}\exp\left(-\frac{E_V{}^M}{kT}\right)\times\left\{1+16C_1\exp\left(\frac{B_2}{kT}\right)\right\}. \tag{16}$$

From Eqs. (11) and (10),

$$C_1=\tfrac{1}{16}\exp\left(-\frac{B_2}{kT}\right)\left\{\left(1+32C_t\exp\left(\frac{B_2}{kT}\right)\right)^{1/2}-1\right\}. \tag{17}$$

Equation (16) can be written as

$$\left(\frac{dT}{dt}\right)=-\frac{14\nu_1kT^2}{B_2}\exp\left(-\frac{E_V{}^M+B_2}{kT}\right)\times\left\{1+32C_t\exp\left(\frac{B_2}{kT}\right)\right\}^{1/2}, \tag{18}$$

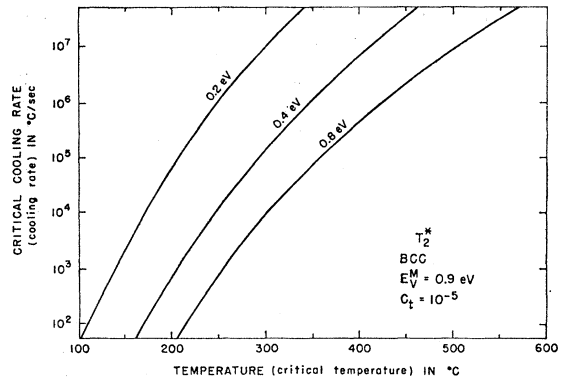

FIG. 9. The values of the critical cooling rate for the formation of divacancies at various temperatures for $E_V{}^M=0.9$ eV. This figure can be directly used for the relation between the cooling rate and the ciritical temperature. Iron is close to this case.

If one knows ν_1, $E_V{}^M$, B_2, and C_t, the value of the right side of Eq. (18) can be calculated as a function of temperature T. At any temperature T, dT/dt can be calculated; this will be called the "critical cooling rate." If the specimen is cooled slower than the critical cooling rate, the thermal equilibrium between single vacancies and divacancies is maintained. If the cooling rate is faster than the critical cooling rate, single vacancies move too slow to maintain the thermal equilibrium between single vacancies and divacancies. When the cooling rate is known, the critical temperature T^* can be calculated. Above T^* thermal equilibrium between single vacancies and divacancies is maintained but below T^* single vacancies move too slow to maintain the thermal equilibrium between single vacancies and divacancies and the situation at T^* is preserved.

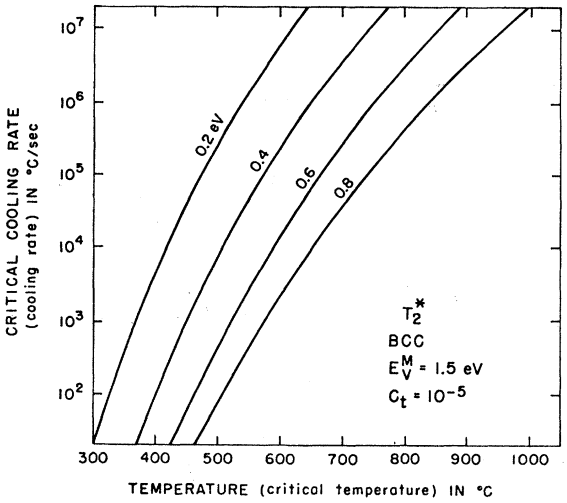

FIG. 10. The values of the ciritical cooling rate for the formation of divacancies at various temperatures for $E_V{}^M=1.5$ eV. This is also for the plot of the cooling rate versus critical temperature.

At $T=T^*$

$$\left(\frac{dT}{dt}\right)_{T=T^*}=-\frac{14\nu_1 kT^{*2}}{B_2}\exp\left(-\frac{E_V{}^M+B_2}{kT^*}\right)\times\left\{1+32C_t\exp\left(\frac{B_2}{kT^*}\right)\right\}^{1/2}. \quad (19)$$

The values of the critical cooling rate at various temperatures for $E_V{}^M=0.9$ eV are given in Fig. 9. ν_1 and C_t are taken to be 10^{13} sec^{-1} and 10^{-5}, respectively. This case is somewhat similar to the case for iron. The values of the critical cooling rate at various temperatures for body centered metals having $E_V{}^M=1.5$ eV and $E_V{}^M=2.0$ eV are also plotted in Figs. 10 and 11, respectively. ν_1 and C_t are also taken to be 10^{13} sec^{-1} and 10^{-5}, respectively. These cases are also somewhat similar to the cases for molybdenum[35] and tungsten,[4] respectively.

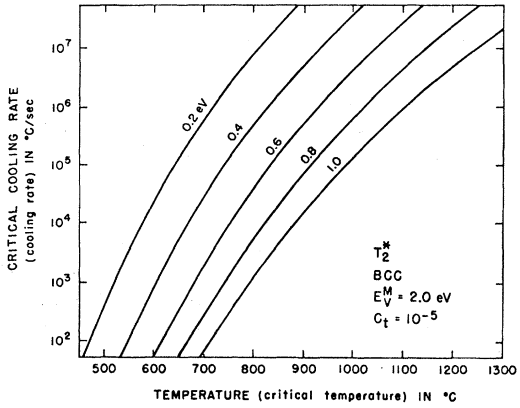

FIG. 11. The values of the critical cooling rate for the formation of divacancies at various temperatures for $E_V{}^M=2.0$ eV. Tish figure can be directly used for the relation between the cooling rate and the critical temperature. Tungsten is close to this case.

E. Divacancy Formation During Annealing

A quenched specimen contains single vacancies and divacancies and the relative concentration can be estimated from the critical temperature T^* as discussed in Sec. V D. The fractional concentration of divacancies $(C_2)_0$ after a quench is

$$(C_2)_0=4(C_1)_0{}^2\exp(B_2/kT^*)=\tfrac{1}{64}\exp\left(-\frac{B_2}{kT^*}\right)\left\{\left[1+32C_t\exp\left(\frac{B_2}{kT^*}\right)\right]^{1/2}-1\right\}^2. \quad (20)$$

[35] J. D. Meakin, A. Lawley, and R. C. Koo, in *Lattice Defects in Quenched Metals*, edited by R. M. J. Cotterill, M. Doyama, J. J. Jackson, and M. Meshii (Academic Press Inc., New York, 1965), p. 767.

When the annealing of vacancies and divacancies into sinks is small and the loss can be neglected, then

$$C_t=C_1+2C_2.$$

Using this equation, Eq. (10) can be integrated.

$$C_1=\frac{\exp\{-(t+t_0)/\tau\}-1+\{1+32C_t\exp(B_2/kT)\}^{1/2}[1+\exp\{-(t+t_0)/\tau\}]}{16[1-\exp\{-(t+t_0)/\tau\}]\exp(B_2/kT)}, \tag{21}$$

where

$$\frac{1}{\tau}=14\nu_1\exp\left(-\frac{E_V{}^M+B_2}{kT}\right)\left\{1+32C_t\exp\left(\frac{B_2}{kT}\right)\right\} \tag{22}$$

$$t_0=\tau\ln\frac{16(C_1)_0\exp(B_2/kT)+1-\{1+32C_t\exp(B_2/kT)\}^{1/2}}{16(C_1)_0\exp(B_2/kT)+1+\{1+32C_t\exp(B_2/kT)\}^{1/2}}. \tag{23}$$

τ has the dimensions of time and is related to how fast the equilibrium divacancies are formed. For iron, $E_V{}^M$ and ν_1 are taken to be 0.9 eV and 10^{13} sec^{-1}, respectively. Figure 12 shows the plot of the values of τ (right scale) in iron for the case $C_t=10^{-5}$, $B_2=0.1$, 0.25, and 0.5 eV. Figure 12 also shows the plot of the values of τ (left scale) for tungsten. $E_V{}^M$ and ν_1 are taken to be 2.0 eV and 10^{13} sec^{-1}. For the case that $C_t=10^{-5}$, $B_2=0.2$, 0.8, and 1.5 the values of τ are calculated.

VI. NEXT-NEAREST-NEIGHBOR INTERACTION

In this section the interaction between atoms up to the next-nearest-neighbor interaction is considered. In body-centered metals the next-nearest-neighbor is only $2/\sqrt{3}=1.16$ times the nearest-neighbor distance. The third neighbor is $(\sqrt{11})/\sqrt{3}=1.91$ times the nearest-neighbor distance.

A. General Kinetic Equations

The kinetic equations for body-centered-cubic pure metals up to the next-nearest-neighbor interactions are

$$\begin{aligned}dC_1/dt=&-2\alpha\{V,V\rightarrow d(\mathrm{I});A\}C_1{}^2+2\alpha\{d(\mathrm{I})\rightarrow V,V;A\}-2\alpha\{V,V\rightarrow d(\mathrm{II});A\}C_1{}^2\\&+2\alpha\{d(\mathrm{II})\rightarrow V,V;A\}-\alpha\{d(\mathrm{I}),V\rightarrow t^{71};A\}C_1C_2{}^{\mathrm{I}}+\alpha\{t^{71}\rightarrow d(\mathrm{I}),V;A\}C_3{}^{71}\\&-\alpha\{d(\mathrm{II}),V\rightarrow t^{71};A_3'\}C_1C_2{}^{\mathrm{II}}+\alpha\{t^{71}\rightarrow d(\mathrm{II}),V;A\}C_3{}^{71}-\alpha\{d(\mathrm{I}),V\rightarrow t^{109};A\}C_1C_2{}^{\mathrm{I}}\\&+\alpha\{t^{109}\rightarrow d(\mathrm{I}),V;A\}C_3{}^{109}-\alpha\{d(\mathrm{II}),V\rightarrow t^{109};A\}C_1C_2{}^{\mathrm{II}}+\alpha\{t^{109}\rightarrow d(\mathrm{II}),V;A\}C_3{}^{109}\\&-\alpha\{d(\mathrm{I}),V\rightarrow t^{180(\mathrm{I})};A\}C_1C_2{}^{\mathrm{I}}+\alpha\{t^{180(\mathrm{I})}\rightarrow d(\mathrm{I}),V;A\}C_3{}^{180(\mathrm{I})}-\alpha\{d(\mathrm{II}),V\rightarrow t^{180(\mathrm{I})};A\}C_1C_2{}^{\mathrm{II}}\\&+\alpha\{t^{180(\mathrm{I})}\rightarrow d(\mathrm{II}),V;A\}C_3{}^{180(\mathrm{I})}-\alpha\{d(\mathrm{I}),V\rightarrow t^{90};A\}C_1C_2{}^{\mathrm{I}}+\alpha\{t^{90}\rightarrow d(\mathrm{I}),V;A\}C_3{}^{90}\\&-\alpha\{d(\mathrm{I}),V\rightarrow t^{144};A\}C_1C_2{}^{\mathrm{I}}+\alpha\{t^{144}\rightarrow d(\mathrm{I}),V;A\}C_3{}^{144}-\alpha\{d(\mathrm{I}),V\rightarrow t^{180(\mathrm{II})};A\}C_1C_2{}^{\mathrm{I}}\\&+\alpha\{t^{180(\mathrm{II})}\rightarrow d(\mathrm{I}),V;A\}C_3{}^{180(\mathrm{II})}-\alpha\{d(\mathrm{I}),V\rightarrow t^{180(\mathrm{II})};A\}C_1C_2{}^{\mathrm{II}}\\&+A\{t^{180(\mathrm{II})}\rightarrow A(\mathrm{I}),V;A\}C_3{}^{180(\mathrm{II})}-\alpha\{V,V,V\rightarrow t^{109};A\}C_1{}^3+3\alpha\{t^{109}\rightarrow V,V,V;A\}C_3{}^{109}\\&-\alpha\{V,V,V\rightarrow t^{90};A\}C_1{}^3+3\alpha\{t^{90}\rightarrow V,V,V;A\}C_3{}^{90}-\alpha\{V,V,V\rightarrow t^{144};A\}C_1{}^3\\&+3\alpha\{t^{144}\rightarrow V,V,V;A\}C_3{}^{144}-\alpha(V,t\rightarrow te;A)C_1C_3+D_1\nabla^2C_1;\end{aligned} \tag{24a}$$

$$\begin{aligned}dC_2{}^{\mathrm{I}}/dt=&\alpha(V,V\rightarrow d(\mathrm{I});A)C_1{}^2-\alpha(d(\mathrm{I})\rightarrow V,V;A)C_2{}^{\mathrm{I}}-\alpha\{d(\mathrm{I}),V\rightarrow t^{71};A\}C_1C_2{}^{\mathrm{I}}\\&+\alpha\{t^{71}\rightarrow d(\mathrm{I}),V;A\}C_3{}^{71}-\alpha\{d(\mathrm{I}),V\rightarrow t^{109};A\}C_1C_2{}^{\mathrm{I}}+\alpha\{t^{109}\rightarrow d(\mathrm{I}),V;A\}C_3{}^{109}\\&-\alpha\{d(\mathrm{I}),V\rightarrow t^{180(\mathrm{I})};A\}C_1C_2{}^{\mathrm{I}}+\alpha\{t^{180(\mathrm{I})}\rightarrow d(\mathrm{I}),V;A\}C_3{}^{180(\mathrm{I})}-\alpha\{d(\mathrm{I}),V\rightarrow t^{90};A\}C_1C_2{}^{\mathrm{I}}\\&+\alpha\{t^{90}\rightarrow d(\mathrm{I}),V;A\}C_3{}^{90}-\alpha\{d(\mathrm{I}),V\rightarrow t^{144};A\}C_1C_2{}^{\mathrm{I}}+\alpha\{t^{144}\rightarrow d(\mathrm{I}),V;A\}C_3{}^{144}\\&-\alpha\{d(\mathrm{I}),V\rightarrow t^{180(\mathrm{II})};A\}C_1C_2{}^{\mathrm{I}}+\alpha\{t^{180(\mathrm{II})}\rightarrow d(\mathrm{I}),V;A\}C_3{}^{180(\mathrm{II})}\\&-\alpha\{d(\mathrm{I}),d(\mathrm{I})\rightarrow te;A\}C_2{}^2+D_2\nabla^2C_2{}^{\mathrm{I}},\end{aligned} \tag{24b}$$

$$\begin{aligned}dC_2{}^{\mathrm{II}}/dt=&\alpha(V,V\rightarrow d(\mathrm{II});A)C_1{}^2-\alpha\{d(\mathrm{II})\rightarrow V,V;A\}C_2{}^{\mathrm{II}}-\alpha\{d(\mathrm{II}),V\rightarrow t^{71};A\}C_1C_2{}^{\mathrm{II}}\\&+\alpha\{t^{71}\rightarrow d(\mathrm{II}),V;A\}C_3{}^{71}-\alpha\{d(\mathrm{II}),V\rightarrow t^{109};A\}C_1C_2{}^{\mathrm{II}}+\alpha\{t^{109}\rightarrow d(\mathrm{II}),V;A\}C_3{}^{109}\\&-\alpha\{d(\mathrm{II}),V\rightarrow t^{180(\mathrm{I})};A\}C_1C_2{}^{\mathrm{II}}+\alpha\{t^{180(\mathrm{I})}\rightarrow d(\mathrm{II}),V;A\}C_3{}^{180(\mathrm{I})}-\alpha\{d(\mathrm{II}),V\rightarrow t^{90};A\}C_1C_2{}^{\mathrm{II}}\\&+\alpha\{t^{90}\rightarrow d(\mathrm{II}),V;A\}C_3{}^{90}-\alpha\{d(\mathrm{II}),V\rightarrow t^{180(\mathrm{II})};A\}C_1C_2{}^{\mathrm{II}}+\alpha\{t^{180(\mathrm{II})}\rightarrow d(\mathrm{II}),V;A\}C_3{}^{180(\mathrm{II})}\\&-\alpha\{d(\mathrm{II}),d(\mathrm{II})\rightarrow te;A\}C_2{}^2+D_2\nabla^2C_2{}^{\mathrm{II}}.\end{aligned} \tag{24c}$$

Similarly

$$\frac{dC^{71}}{dt}, \frac{dC^{109}}{dt}, \frac{dC^{180(\mathrm{I})}}{dt}, \frac{dC^{90}}{dt}, \frac{dC^{144}}{dt}, \text{ and } \frac{dC^{180(\mathrm{II})}}{dt}$$

can be easily obtained. In these equations C_1 is the fractional concentration of single vacancies, C_2^{I} and C_2^{II} are the fractional concentrations of type-I and type-II divacancies, respectively. C_3^{71} is the fractional concentration of 71° trivacancies, C_3^{109} is the fractional concentration of 109° trivacancies, $C_3^{180(\mathrm{I})}$ is the fractional concentration of 180°(I) trivacancies, C_3^{90}, C_3^{144}, and $C_3^{180(\mathrm{II})}$ are the fractional concentrations of 90° trivacancies, 144° trivacancies, and 180°(II) trivacancies, respectively. Rate constants α are given in Table III.

B. Kinetic Equations for the Reaction between Single Vacancies and Divacancies

The kinetic equations between the fractional concentration of single vacancies and divacancies of type I and type II are as follows:

$$\frac{\partial C_1}{\partial t}=-112C_1^2\nu\exp\left(-\frac{E_V^M}{kT}\right)+16\nu C_{2A}^{\mathrm{I}}\exp\left(-\frac{B_2^{\mathrm{I}}+E_V^M}{kT}\right)+16\nu C_2^{\mathrm{II}}\exp\left(-\frac{B_2^{\mathrm{II}}+E_V^M}{kT}\right)-D_1\left\{\frac{\partial^2 C_1}{\partial r^2}+\frac{1}{r}\frac{\partial C_1}{\partial r}\right\}; \quad (25a)$$

$$\frac{\partial C_2^{\mathrm{I}}}{\partial t}=-6\nu C_2^{\mathrm{I}}\exp\left(-\frac{B_2^{\mathrm{I}}-B_2^{\mathrm{II}}+E_{2\mathrm{I}}^M}{kT}\right)-8\nu C_2^{\mathrm{I}}\exp\left(-\frac{B_2^{\mathrm{I}}+E_V^M}{kT}\right)+32\nu C_1^2\exp\left(-\frac{E_V^M}{kT}\right)+8\nu C_2^{\mathrm{II}}\exp\left(-\frac{E_{2\mathrm{I}}^M}{kT}\right)-D_{2\mathrm{I}}\left\{\frac{\partial^2 C_2^{\mathrm{I}}}{\partial r^2}+\frac{1}{r}\frac{\partial C_2^{\mathrm{II}}}{\partial r}\right\}; \quad (25b)$$

$$\frac{\partial C_2^{\mathrm{II}}}{\partial t}=6\nu C_2^{\mathrm{I}}\exp\left(-\frac{B_2^{\mathrm{I}}-B_2^{\mathrm{II}}+E_{2\mathrm{I}}^M}{kT}\right)-8\nu C_2^{\mathrm{II}}\exp\left(-\frac{B_2^{\mathrm{II}}+E_V^M}{kT}\right)+24\nu C_1^2\exp\left(-\frac{E_V^M}{kT}\right)-8\nu C_2^{\mathrm{II}}\exp\left(-\frac{E_{2\mathrm{I}}^M}{kT}\right)-D_{2\mathrm{II}}\left\{\frac{\partial^2 C_{2\mathrm{II}}}{\partial r^2}+\frac{1}{r}\frac{\partial C_2^{\mathrm{I}}}{\partial r}\right\}, \quad (25c)$$

where C_1, C_2^{I}, and C_2^{II} are the fractional concentrations of single vacancies, type-I divacancies, and type-II divacancies, respectively; ν is the frequency of vibration of the atom next to a vacancy. Here all of the frequency coefficients are taken to be the same for simplicity. D_1, $D_{2\mathrm{I}}$, and $D_{2\mathrm{II}}$ are the diffusion constants associated with the motion of single vacancies, type-I divacancies, and type-II divacancies, respectively. E_V^M is the activation energy for the migration of a single vacancy. $E_{2\mathrm{I}}^M$ is the activation energy for the migration of a divacancy from type I to type II. B_2^{I} and B_2^{II} are the binding energy of type-I divacancy and type-II divacancy, respectively. r is the distance from a sink. The geometrical constants are derived as follows: In Eq. (25b) the first term is the breakup of type-I divacancies to type-II divacancies. Each of two vacant sites has three ways to break up to type II (3×2). The second term is the breakup of type-I divacancies into single vacancies. Each of the vacant sites has four ways to break up to single vacancies (4×2). The third term is the formation of type-I divacancy by two single vacancies. A single vacancy has eight nearest neighbors, each of whose sites forms a type-I divacancy. For each of the sites there are four possible sites from which a type-I divacancy can be formed (8×4). The fourth term is the formation of type I divacancies from type-II divacancies (4×2). Similarly the first term of Eq. (25c) is the formation of type-II divacancies from type-I divacancies. The second term is the breakup of type-II divacancies to single vacancies (4×2). The third term is the formation of type-II divacancies from single vacancies (8×3). The fourth term is the formation of type-I divacancies from type-II divacancies. The diagram for the energy relation is plotted in Fig. 13.

C. Thermal Equilibrium

At thermal equilibrium the formation and breakup of divacancies are equal. The left side of Eqs. (25a), (25b), and (25c) are all zero. Therefore,

$$C_2^{\mathrm{I}}=\xi_{\mathrm{I}}C_1^2 \quad (26)$$

and

$$C_2^{\mathrm{II}}=\xi_{\mathrm{II}}C_1^2, \quad (27)$$

TABLE III. The rate constants of the kinetic equations between defects for the next-nearest-neighbor interaction.

		Reaction	Constants
I		$V \rightarrow V$	$\alpha_1(V \rightarrow V; A) = 8\nu_1 \exp(-E_V{}^M/kT)$
II	1	$d(\mathrm{I}) \rightarrow d(\mathrm{II})$	$\alpha_1(d(\mathrm{I}) \rightarrow d(\mathrm{II}); A_{2\mathrm{I}}) = 6_{\mathrm{I}}\nu_2 \exp\{-(E_{2\mathrm{I}}{}^M + B_d{}^{\mathrm{I}} - B_d{}^{\mathrm{II}})/kT\}$
	2	$d(\mathrm{II}) \rightarrow d(\mathrm{I})$	$\alpha_1(d(\mathrm{II}) \rightarrow d(\mathrm{I}); A_{2\mathrm{II}}) = 8_{\mathrm{II}}\nu_2 \exp\{-(E_{2\mathrm{II}}{}^M + B_d{}^{\mathrm{II}} - B_d{}^{\mathrm{I}})/kT\}$
	3	$d(\mathrm{I}) \rightarrow V+V$	$\alpha_1(d(\mathrm{I}) \rightarrow V, V; A) = 8\nu_1 \exp\{-(E_V{}^M + B_d{}^{\mathrm{I}})/kT\}$
	4	$d(\mathrm{II}) \rightarrow V+V$	$\alpha_1(d(\mathrm{II}) \rightarrow V, V; A) = 8\nu_1 \exp\{-(E_V{}^M + B_d{}^{\mathrm{II}})/kT\}$
III	1	$t^{71} \rightarrow t^{71}$	$\alpha_1(t^{71} \rightarrow t^{71}; A_{2\mathrm{I}}) = 4_{\mathrm{I}}\nu_2 \exp\{-E_{2\mathrm{I}}{}^M/kT\}$
	2	$t^{71} \rightarrow t^{109}$	$\alpha_1(t^{71} \rightarrow t^{109}; A) = 2\nu_1 \exp\{-(E_V{}^M + B_t{}^{71} - B_t{}^{109})kT\}$
	3	$t^{71} \rightarrow t^{90}$	$\alpha_1(t^{71} \rightarrow t^{90}; A) = 4\nu_1 \exp\{-(E_V{}^M + B_t{}^{71} - B_t{}^{90})/kT\}$
	4	$t^{71} \rightarrow d(\mathrm{I}) + V$	$\alpha_1(t^{71} \rightarrow d(\mathrm{I}), V; A) = 6\nu_1 \exp\{-(E_V{}^M + B_t{}^{71} - B_d{}^{\mathrm{I}})/kT\}$
	5	$t^{71} \rightarrow d(\mathrm{II}) + V$	$\alpha_1(t^{71} \rightarrow d(\mathrm{I}), V; A) = 2\nu_1 \exp\{-(E_V{}^M + B_t{}^{71} - B_d{}^{\mathrm{II}})/kT\}$
	6	$t^{71} \rightarrow t^{144}$	$\alpha_1(t^{71} \rightarrow t^{144}; A_{2\mathrm{I}}) = 2_{\mathrm{I}}\nu_2 \exp\{-(E_{2\mathrm{I}}{}^M + B_t{}^{71} - B_t{}^{144})/kT\}$
IV	1	$t^{109} \rightarrow t^{71}$	$\alpha_1(t^{109} \rightarrow t^{71}; A_{2\mathrm{I}}) = 2_{\mathrm{I}}\nu_2 \exp\{-(E_{2\mathrm{I}}{}^M + B_t{}^{109} - B_t{}^{71})/kT\}$
	2	$t^{109} \rightarrow t^{144}$	$\alpha_1(t^{109} \rightarrow t^{144}; A_{2\mathrm{I}}) = 2_{\mathrm{I}}\nu_2 \exp\{-(E_{2\mathrm{I}}{}^M + B_t{}^{109} - B_t{}^{144})/kT\}$
	3	$t^{109} \rightarrow t^{90}$	$\alpha_1(t^{109} \rightarrow t^{90}; A_3) = 2\nu_3 \exp\{-(E_3{}^M + B_t{}^{109} - B_t{}^{90})/kT\}$
	4	$t^{109} \rightarrow d(\mathrm{I}) + V$	$\alpha_1(t^{109} \rightarrow d(\mathrm{I}), V; A) = 10\nu_1 \exp\{-(E_V{}^M + B_t{}^{109} - B_d{}^{\mathrm{I}})/kT\}$
	5	$t^{109} \rightarrow d(\mathrm{II}) + V$	$\alpha_1(t^{109} \rightarrow d(\mathrm{II}), V; A) = 2\nu_1 \exp\{-(E_V{}^M + B_t{}^{109} - B_d{}^{\mathrm{II}})/kT\}$
	6	$t^{109} \rightarrow V+V+V$	$\alpha_1(t^{109} \rightarrow V, V, V; A) = 2\nu_1 \exp\{-(E_V{}^M + B_d{}^{109})/kT\}$
V	1	$t^{180}(\mathrm{I}) \rightarrow t^{144}$	$\alpha_1(t^{180}(\mathrm{I}) \rightarrow t^{144}; A_{2\mathrm{I}}) = 4_{\mathrm{I}}\nu_2 \exp\{-(E_{2\mathrm{I}}{}^M + B^{180(\mathrm{I})} - B^{144})/kT\}$
	2	$t^{180}(\mathrm{I}) \rightarrow d(\mathrm{I}) + V$	$\alpha_1(t^{180}(\mathrm{I}) \rightarrow d(\mathrm{I}), V; A) = 8\nu_1 \exp\{-(E_V{}^M + B_t{}^{180(\mathrm{I})} - B_d{}^{\mathrm{I}})/kT\}$
	3	$t^{180}(\mathrm{I}) \rightarrow d(\mathrm{II}) + V$	$\alpha_1(t^{180}(\mathrm{I}) \rightarrow d(\mathrm{II}), V; A) = 8\nu_1 \exp\{-(E_V{}^M + B_t{}^{180(\mathrm{I})} - B_d{}^{\mathrm{II}})/kT\}$
VI	1	$t^{90} \rightarrow t^{71}$	$\alpha_1(t^{90} \rightarrow t^{71}; A_3{}^{90}) = 4_{\ 90}\nu_3 \exp\{-({}_{90}E_3{}^M + B_t{}^{90} - B_t{}^{71})/kT\}$
	2	$t^{90} \rightarrow t^{109}$	$\alpha_1(t^{90} \rightarrow t^{109}; A_3{}^{90}) = 2_{\ 90}\nu_3 \exp\{-({}_{90}E_3{}^M + B_t{}^{90} - B_t{}^{109})/kT\}$
	3	$t^{90} \rightarrow t^{144}$	$\alpha_1(t^{90} \rightarrow t^{144}; A_{1\mathrm{I}}) = 4_{\mathrm{I}}\nu_2 \exp\{-(E_{2\mathrm{I}}{}^M + B_t{}^{90} - B_t{}^{144})/kT\}$
	4	$t^{90} \rightarrow d(\mathrm{I}) + V$	$\alpha_1(t^{90} \rightarrow d(\mathrm{I}), V; A) = 8\nu_1 \exp\{-(E_V{}^M + B_t{}^{90} - B_d{}^{\mathrm{I}})/kT\}$
	5	$t^{90} \rightarrow d(\mathrm{II}) + V$	$\alpha_1(t^{90} \rightarrow d(\mathrm{II}), V; A) = 4\nu_1 \exp\{-(E_V{}^M + B_t{}^{90} - B_d{}^{\mathrm{II}})/kT\}$
	6	$t^{90} \rightarrow V+V+V$	$\alpha_1(t^{90} \rightarrow V, V, V; A) = 2\nu_1 \exp\{-(E_V{}^M + B_t{}^{90})/kT\}$
VII	1	$t^{144} \rightarrow t^{144}$	$\alpha_1(t^{144} \rightarrow t^{144}; A_3{}^{144}) = {}_{144}\nu_3 \exp\{-{}_{144}E_3{}^M/kT\}$
	2	$t^{144} \rightarrow t^{71}$	$\alpha_1(t^{144} \rightarrow t^{71}; A_3{}^{144}) = 2_{\ 144}\nu_3 \exp\{-({}_{144}E_3{}^M + B_t{}^{144} - B_t{}^{71})/kT\}$
	3	$t^{144} \rightarrow t^{109}$	$\alpha_1(t^{144} \rightarrow t^{109}; A_{2\mathrm{II}}) = 4_{\mathrm{II}}\nu_2 \exp\{-({}_{\mathrm{II}}E_2{}^M + B_t{}^{144} - B_t{}^{109})/kT\}$
	4	$t^{144} \rightarrow t^{180}(\mathrm{I})$	$\alpha_1(t^{144} \rightarrow t^{180}(\mathrm{I}); A_{2\mathrm{II}}) = 2_{\mathrm{II}}\nu_2 \exp\{-({}_{\mathrm{II}}E_2{}^M + B_t{}^{144} - B_t{}^{180(\mathrm{I})})/kT\}$
	5	$t^{144} \rightarrow d(\mathrm{I}) + V$	$\alpha_1(t^{144} \rightarrow d(\mathrm{I}), V; A) = 8\nu_1 \exp\{-(E_V{}^M + B_t{}^{144} - B_d{}^{\mathrm{I}})/kT\}$ $\alpha_1(t^{144} \rightarrow d(\mathrm{I}), V; A_{2\mathrm{I}}) = 2_{\mathrm{I}}\nu_2 \exp\{-({}_{\mathrm{I}}E_2{}^M + B_t{}^{144} - B_d{}^{\mathrm{I}})/kT\}$ $\alpha_1(t^{144} \rightarrow d(\mathrm{I}), V; A_{2\mathrm{II}}) = 3_{\mathrm{II}}\nu_2 \exp\{-({}_{\mathrm{II}}E_2{}^M + B_t{}^{144} - B_d{}^{\mathrm{I}})/kT\}$
	6	$t^{144} \rightarrow V+V+V$	$\alpha_1(t^{144} \rightarrow V, V, V; A) = \nu_1 \exp\{-(E_V{}^M + B_t{}^{144})/kT\}$
VIII	1	$t^{180}(\mathrm{II}) \rightarrow t^{144}$	$\alpha_1(t^{180}(\mathrm{II}) \rightarrow t^{144}; A_{2\mathrm{II}}) = 8_{\mathrm{II}}\nu_2 \exp\{-({}_{\mathrm{II}}E_2{}^M + B_d{}^{180(\mathrm{II})} - B^{144})/kT\}$
	2	$t^{180}(\mathrm{II}) \rightarrow d(\mathrm{I}) + V$	$\alpha_1(t^{180}(\mathrm{II}) \rightarrow d(\mathrm{I}), V; A_{2\mathrm{II}}) = 8_{\mathrm{II}}\nu_2 \exp\{-({}_{\mathrm{II}}E_2{}^M + B_d{}^{180(\mathrm{II})} - B_d{}^{\mathrm{I}})/kT\}$
	3	$t^{180}(\mathrm{II}) \rightarrow d(\mathrm{II}) + V$	$\alpha_1(t^{180}(\mathrm{II}) \rightarrow d(\mathrm{II}), V; A) = 8\nu_1 \exp\{-(E_V{}^M + B_d{}^{180(\mathrm{II})} - B_d{}^{\mathrm{II}})/kT\}$
IX	1	$d(\mathrm{I}) + V \rightarrow t^{71}$	$\alpha_1(d(\mathrm{I}), V \rightarrow t^{71}; A) = 24\nu \exp\{-(E^M + B_d{}^{\mathrm{I}} - B_t{}^{71})/kT\}$
	2	$d(\mathrm{I}) + V \rightarrow t^{109}$	$\alpha_1(d(\mathrm{I}), V \rightarrow t^{109}; A) = 24\nu \exp\{-(E_V{}^M + B_d{}^{\mathrm{I}} - B_t{}^{109})/kT\}$
	3	$d(\mathrm{I}) + V \rightarrow t^{180(\mathrm{I})}$	$\alpha_1(d(\mathrm{I}), V \rightarrow t^{180(\mathrm{I})}; A) = 8\nu_1 \exp\{-(E_V{}^M + B_d{}^{\mathrm{I}} - B_t{}^{180(\mathrm{I})})/kT\}$
	4	$d(\mathrm{I}) + V \rightarrow t^{144}$	$\alpha_1(d(\mathrm{I}), V \rightarrow t^{144}; A) = 16\nu_1 \exp\{-(E_V{}^M + B_d{}^{\mathrm{I}} - B_t{}^{144})/kT\}$
	5	$d(\mathrm{I}) + V \rightarrow t^{90}$	$\alpha(d(\mathrm{I}), V \rightarrow t^{90}; A) = 24\nu_1 \exp\{-(E_V{}^M + B_d{}^{\mathrm{I}} - B_t{}^{90})/kT\}$
X	1	$d(\mathrm{II}) + V \rightarrow t^{71}$	$\alpha_1(d(\mathrm{II}), V \rightarrow t^{71}; A_3{}') = 8\nu_3{}' \exp\{-(E_3{}'{}^M + B_d{}^{\mathrm{II}})/kT\}$
	2	$d(\mathrm{II}) + V \rightarrow t^{180(\mathrm{II})}$	$\alpha_1(d(\mathrm{II}), V \rightarrow t^{180(\mathrm{II})}; A) = 8\nu_1 \exp\{-(E_V{}^M + B_d{}^{\mathrm{II}} - B_t{}^{180(\mathrm{II})}/kT\}$
	3	$d(\mathrm{II}) + V \rightarrow t^{144}$	$\alpha_1(d(\mathrm{II}), V \rightarrow t^{144}; A) = 10\nu_1 \exp\{-(E_V{}^M + B_d{}^{\mathrm{II}} - B_t{}^{144})/kT\}$
	4	$d(\mathrm{II}) + V \rightarrow t^{180(\mathrm{I})}$	$\alpha_1(d(\mathrm{II}), V \rightarrow t^{180(\mathrm{I})}; A) = 16\nu_3 \exp\{-E_3{}^M + B_d{}^{\mathrm{II}} - B_t{}^{180(\mathrm{II})}/kT\}$
	5	$d(\mathrm{II}) + V \rightarrow t^{90}$	$\alpha_1(d(\mathrm{II}), V \rightarrow t^{90}; A) = 32\nu_1 \exp\{-(E_V{}^M + B_d{}^{\mathrm{II}} - B_t{}^{90})/kT\}$
XI	1	$V+V+V \rightarrow t^{109}$	$\alpha(V, V, V \rightarrow t^{109}; A) = 4\nu_1 \exp\{-E_V{}^M/kT\}$
	2	$V+V+V \rightarrow t^{144}$	$\alpha(V, V, V \rightarrow t^{144}; A) = 2\nu_1 \exp\{-E_V{}^M/kT\}$
	3	$V+V+V \rightarrow t^{90}$	$\alpha(V, V, V \rightarrow t^{90}; A) = 4\nu_1 \exp\{-E_V{}^M/kT\}$
XII	1	$V+V \rightarrow d(\mathrm{I})$	$\alpha_1(V, V \rightarrow d(\mathrm{I}); A) = 32\nu_1 \exp(-E_V{}^M/kT)$
	2	$V+V \rightarrow d(\mathrm{II})$	$\alpha_1(V, V \rightarrow d(\mathrm{II}); A) = 24\nu_1 \exp(-E_V{}^M/kT)$

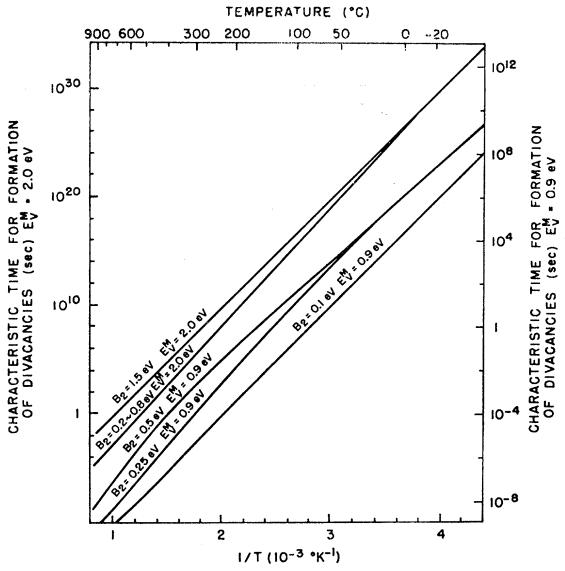

FIG. 12. The plot of characteristic time τ for the formation of divacancies in body-centered-cubic metals during annealing at various temperatures. Total concentration of voids was chosen to be 10^{-5}. For the case $E_M{}^V=0.9$ eV ($B_2=0.1$, 0.25, and 0.5 eV), the values of τ are plotted. For this case, use the scale on the left. This case is close to iron. For the case $E_M{}^V=2.0$ eV ($B_2=0.2$–0.8 eV and $B_2=1.5$ eV) the values of τ in seconds are plotted. Use the scale on the right. This case is close to tungsten.

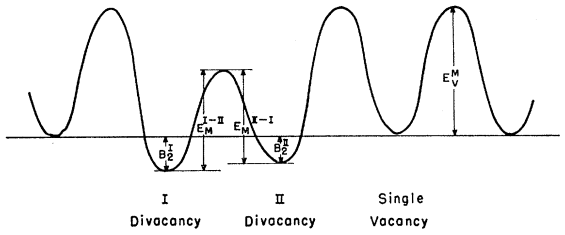

FIG. 13. Schematic diagram for the energy relation of a single vacancy, a divacancy type I and a divacancy type II and their motion.

where

$$\xi_I=4\exp(B_2{}^I/kT), \tag{28}$$

$$\xi_{II}=3\exp(B_2{}^{II}/kT). \tag{29}$$

Let the total fractional concentration C_t of single vacancies C_1 and divacancies ($C_2{}^I$ and $C_2{}^{II}$) be C_t, then

$$C_t=C_1+2C_2{}^I+2C_2{}^{II}. \tag{30}$$

From Eqs. (26), (27), and (30)

$$C_1=\frac{[1+8(\xi_I+\xi_{II})C_t]^{1/2}-1}{4(\xi_I+\xi_{II})}, \tag{31}$$

$$C_2{}^I=\left(\frac{[1+8(\xi_I+\xi_{II})C_t]^{1/2}-1}{4(\xi_I+\xi_{II})}\right)^2\xi_I, \tag{32}$$

$$C_2{}^{II}=\left(\frac{[1+8(\xi_I+\xi_{II})C_t]^{1/2}-1}{4(\xi_I+\xi_{II})}\right)^2\xi_{II}. \tag{33}$$

The fractional concentrations C_1, $C_2{}^I$, and $C_2{}^{II}$ are plotted in Figs. 14 and 15 for the cases where $C_t=10^{-5}$ and 10^{-6}, respectively. $B_2{}^I$ was taken to be 0.1 and 0.25 eV. $B_2{}^{II}$ was taken to be $0.8B_2{}^I$. In Fig. 16 the fractional concentrations of C_1 and $C_2{}^I$ are plotted. In Fig. 17 $C_2{}^{II}$ is plotted. In these cases, $B_2{}^I$ was taken to be 0.4 eV and the total fractional concentration of voids was taken to be 10^{-5}. In these figures, various values of $B_2{}^{II}$ are taken. If $B_2{}^{II}$ is taken to be zero and ξ_{II} can

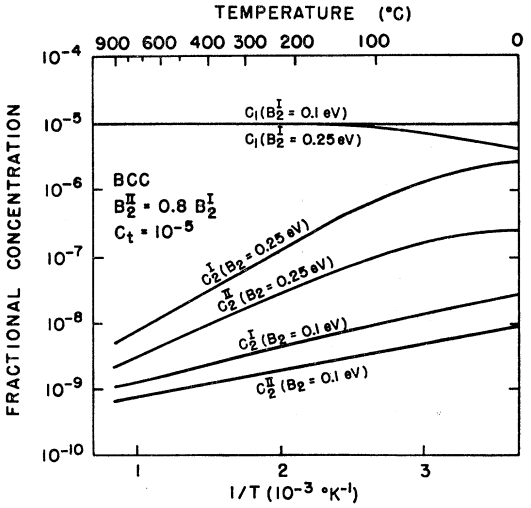

FIG. 14. Equilibrium fractional concentrations of single vacancies, divacancies (type I and II) at various temperatures. The total fractional void concentration was chosen to be 10^{-5}, and $B_2{}^{II}$ is taken to be $0.8B_2{}^I$. This plot is independent of the activation energy for motion and the formation energy of a vacancy. Therefore, Figs. 14 and 15 can be used for any body-centered cubic metals.

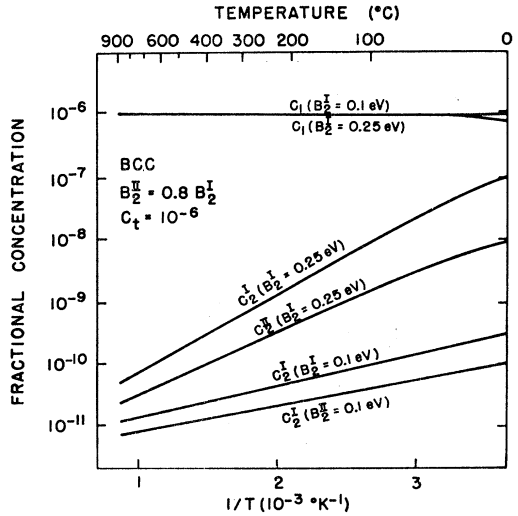

FIG. 15. Equilibrium fractional concentrations of single vacancies, divacancies (type I and II) at various temperatures. The total fractional void concentration was chosen to be 10^{-6}, and $B_2{}^{II}$ is taken to be $0.8B_2{}^I$. This plot is independent of the activation energy for motion and the formation energy of a vacancy.

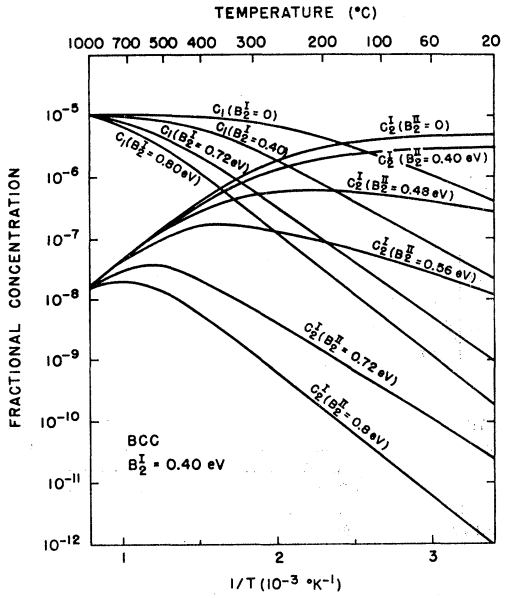

FIG. 16. The equilibrium fractional concentrations of single vacancies and type-I divacancies versus the reciprocal of temperature. B_2^{I} was taken to be 0.40 eV. B_2^{II} was varied and shown in the figure. The total fractional concentration of voids was chosen to be 10^{-5}. This plot is also independent of the activation energy for motion and the formation energy of a vacancy.

be ignored with respect to ξ_{I} then Eq. (26) becomes Eq. (4) and Eq. (32) becomes Eq. (20).

D. Divacancy Formation During Quenching

The formation of divacancies during quenching can be treated as discussed in Sec. V D. The kinetic equation between single vacancies and type-I divacancies is

$$\frac{dC_1}{dt}=-64C_1^2\nu_1\exp\left(-\frac{E_M{}^V}{kT}\right)+16\nu_1C_2{}^{\mathrm{I}}\exp\left(-\frac{E_M{}^V+B_2{}^{\mathrm{I}}}{kT}\right). \quad (34)$$

The kinetic equation between single vacancies and type-II divacancies is

$$\frac{dC_1}{dt}=-48C_1^2\nu_1\exp\left(-\frac{E_M{}^V}{kT}\right)+16\nu_1C_2{}^{\mathrm{II}}\exp\left(-\frac{E_M{}^V+B_2{}^{\mathrm{II}}}{kT}\right). \quad (35)$$

Here ν_2 is taken to be equal to ν_1. Since it is assumed that no vacancies anneal during quenching

$$C_t=\text{const.}=C_1+2C_2{}^{\mathrm{I}}+2C_2{}^{\mathrm{II}}. \quad (30)$$

Differentiating Eqs. (26), (27), and (30) with respect to time t

$$\frac{dC_2{}^{\mathrm{I}}}{dt}=2C_1\xi_{\mathrm{I}}\frac{dC_1}{dt}+\xi_{\mathrm{I}}'C_1^2\frac{dT}{dt}, \quad (36)$$

$$\frac{dC_2{}^{\mathrm{II}}}{dt}=2C_1\xi_{\mathrm{II}}\frac{dC_1}{dt}+\xi_{\mathrm{II}}'C_1^2\frac{dT}{dt}, \quad (37)$$

$$\frac{dC_1}{dt}+2\frac{dC_2{}^{\mathrm{I}}}{dt}+2\frac{dC_2{}^{\mathrm{II}}}{dt}=0, \quad (38)$$

where

$$\xi_{\mathrm{I}}'=-\frac{4B_2{}^{\mathrm{I}}}{kT^2}\exp\left(\frac{B_2{}^{\mathrm{I}}}{kT}\right) \quad (39)$$

$$\xi_{\mathrm{II}}'=-\frac{3B_2{}^{\mathrm{II}}}{kT^2}\exp\left(\frac{B_2{}^{\mathrm{II}}}{kT}\right). \quad (40)$$

Here the ξ''s are the derivatives of the ξ's with respect to temperature T. Adding Eqs. (36) and (37) and using Eq. (38) we obtain

$$\frac{dT}{dt}=-\frac{\frac{1}{2}+2C_1(\xi_{\mathrm{I}}+\xi_{\mathrm{II}})}{C_1^2(\xi_{\mathrm{I}}'+\xi_{\mathrm{II}}')}\frac{dC_1}{dt}. \quad (41)$$

If we assume here that type-I divacancies are always in thermal equilibrium with type-II divacancies during quenching, then the change of single vacancies can be

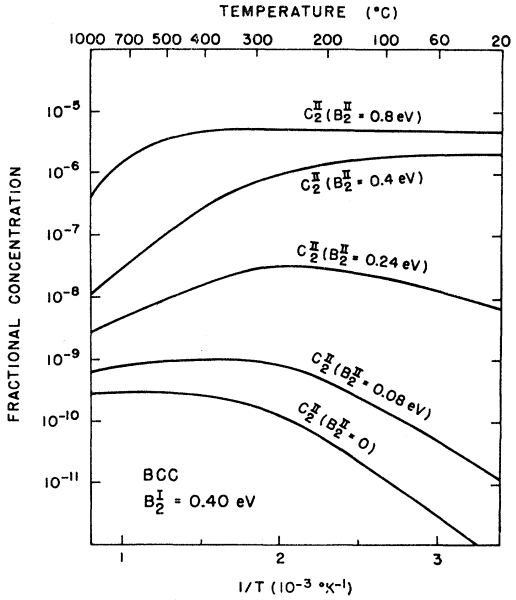

FIG. 17. The equilibrium fractional concentrations of type-II divacancies versus the reciprocal of temperature. $B_2{}^{\mathrm{I}}$ was taken to be 0.40 eV. $B_2{}^{\mathrm{II}}$ was varied and shown in the figure. The total fractional concentration of voids was chosen to be 10^{-5}. This plot is also independent of the activation energy for motion and the formation energy of a vacancy.

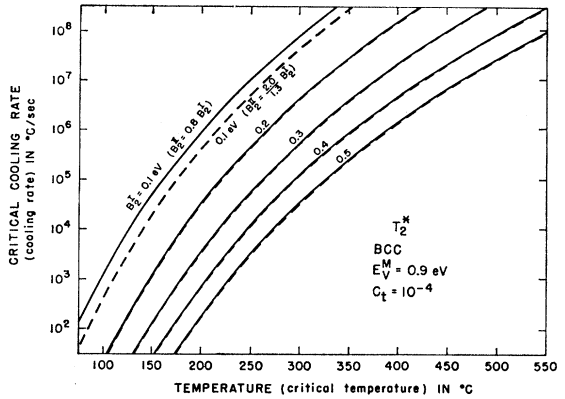

FIG. 18. The values of the critical cooling rate for the formation of divacancies at various temperatures for $E_V{}^M=0.9$ eV. This figure can be directly used for the relation between the cooling rate and the critical temperature. The total concentration of voids was chosen to be 10^{-4}. This case is close to iron. The ratio $B_2{}^{II}/B_2{}^I$ was changed, but it was not sensitive for $B_2{}^I>0.2$ eV.

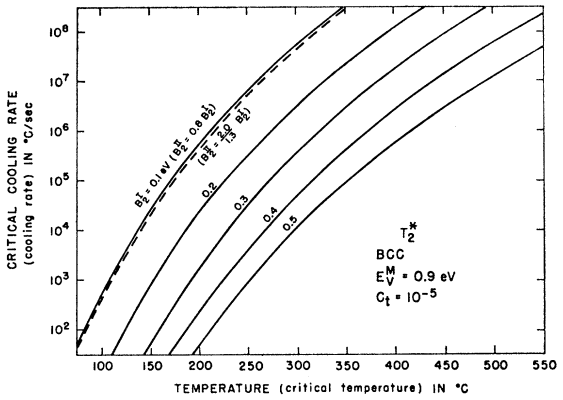

FIG. 19. The values of the critical cooling rate for the formation of divacancies at various temperatures for $E_V{}^M=0.9$ eV. This figure can be directly used for the relation between the cooling rate and the critical temperature. The total concentration of voids was chosen to be 10^{-5}. This case is close to iron. The ratio $B_2{}^{II}/B_2{}^I$ was changed, but it was not sensitive for $B_2{}^I>0.2$ eV.

represented by the sum of the first terms of Eqs. (34) and (35)

$$\frac{dT}{dt}=112\nu_1\exp\left(-\frac{E_M{}^V}{kT}\right)\frac{\frac{1}{2}+2C_1(\xi_I+\xi_{II})}{\xi_I'+\xi_{II}'}$$

$$=56\nu_1\exp\left(-\frac{E_M{}^V}{kT}\right)\frac{[1+8C_t(\xi_I+\xi_{II})]^{1/2}}{\xi_I'+\xi_{II}'}. \quad (42)$$

When one knows ν_1, $E_V{}^M$, $B_2{}^I$, $B_2{}^{II}$, and C_t the value of the right side of Eq. (42) can be calculated as a function of temperature T. At any temperature T, the derivative dT/dt can be calculated; this is the critical cooling rate of this reaction. If the specimen is cooled slower than the critical cooling rate the thermal equilibrium between single vacancies and divacancies is maintained at any temperature T. If the specimen is cooled faster than the critical cooling rate the thermal equilibrium between single vacancies and divacancies is not maintained because single vacancies move too slow to maintain thermal equilibrium at a temperature T. The situation at the temperature T is frozen in. When the cooling rate is known the critical temperature T^* can be calculated. Above T^* single vacancies and divacancies are in thermal equilibrium. Below T^* single vacancies move too slow to maintain thermal equilibrium between single vacancies and divacancies and the situation at T^* is frozen in at $T=T^*$

$$\left(\frac{dT}{dt}\right)_{T=T^*}=\frac{56kT^{*2}\nu_1\exp(-E_M{}^V/kT^*)[1+8C_t\{4\exp(B_2{}^I/kT^*)+3\exp(B_2{}^{II}/kT^*)\}]^{1/2}}{4B_2{}^I\exp(B_2{}^I/kT^*)+3B_2{}^{II}\exp(B_2{}^{II}/kT^*)}. \quad (43)$$

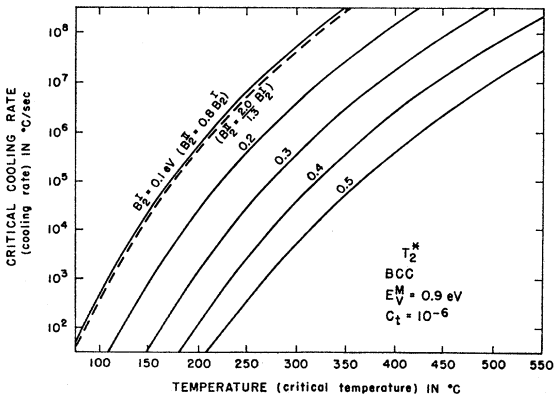

FIG. 20. The values of the critical cooling rate for the formation of divacancies at various temperatures for $E_V{}^M=0.9$ eV. This figure can be directly used for the relation between the cooling rate and the critical temperature. The total concentration of voids was chosen to be 10^{-6}. This is close to iron. The ratio $B_2{}^{II}/B_2{}^I$ was changed, but it was not sensitive for $B_2{}^I>0.2$ eV.

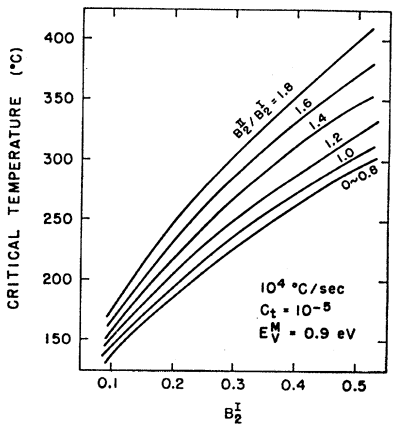

FIG. 21. The critical temperature versus the binding energy of type-I divacancy for the case the total concentration is 10^{-5}, the cooling rate 10^4 °C/sec, and the activation energy for the motion of a single vacancy 0.9 eV. The ratio $B_2{}^{II}/B_2{}^I$ is varied.

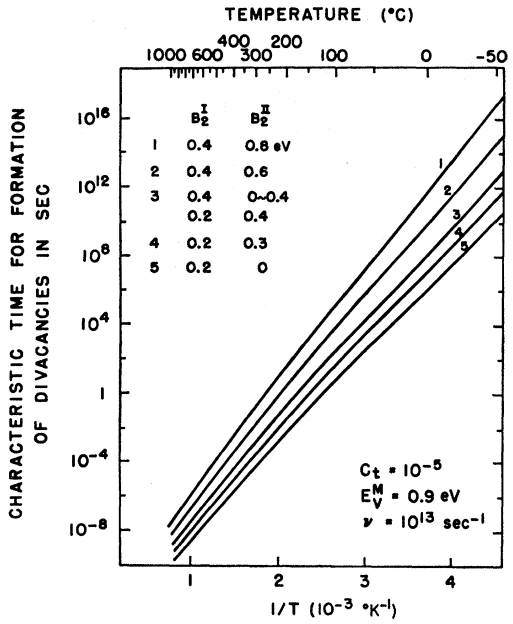

FIG. 22. Characteristic time τ for the formation of divacancies versus the inverse of annealing temperature. The total void concentration, the activation energy for the motion of a single vacancy, and the vibrational frequency were chosen to be 10^{-5}, 0.9 eV, and 10^{13} sec^{-1}, respectively. Each case for the values of the binding energies of type-I, and type-II divacancies are given.

The values of the critical cooling rate at various temperatures for $E_V{}^M=0.9$ eV are plotted in Figs. 18, 19, and 20. ν_1 is taken to be 10^{13} sec^{-1}. The fractional concentrations of total voids are 10^{-4}, 10^{-5}, and 10^{-6} for Figs. 18, 19, and 20, respectively. Solid lines represent $E_2{}^{\mathrm{I}}=0.8E_2{}^{\mathrm{II}}$ and broken lines represent $E_2{}^{\mathrm{I}}=(2.0/1.3)E_2{}^{\mathrm{II}}$. As shown in the figures, if the binding energy of a divacancy is more than 0.2 eV, both cases $[E_2{}^{\mathrm{I}}=0.8E_2{}^{\mathrm{II}}$ and $E_2{}^{\mathrm{I}}=(2.0/1.3)E_2{}^{\mathrm{II}}]$ give almost the same critical temperature. If $B_2{}^{\mathrm{II}}$ is taken to be zero and $3\exp(B_2{}^{\mathrm{II}}/kT^*)$ is ignored compared with $4\exp(B_2{}^{\mathrm{I}}/kT^*)$, Eq. (43) becomes Eq. (19) which is the equation for the nearest-neighbor interaction.

In Fig. 21, the critical temperatures are plotted against $B_2{}^{\mathrm{I}}$ for the case $C_t=10^{-5}$, $dT/dt=10^4$ °C/sec and $E_V{}^M=0.9$ eV. The curves for various values of $B_2{}^{\mathrm{II}}/B_2{}^{\mathrm{I}}$ are shown in the figure.

E. Divacancy Formation During Annealing

We consider the formation of divacancies during annealing as treated in Sec. V E except that in this section the next-nearest-neighbor interaction is taken into account. For simplicity it is again assumed that no vacancies anneal to sinks and that thermal equilibrium is always maintained between type-I and type-II divacancies. The kinetic equation is

$$\frac{dC_1}{dt}=-112C_1{}^2\nu_1\exp\left(-\frac{E_M{}^V}{kT}\right)+16\nu_1C_2{}^{\mathrm{I}}\exp\left(-\frac{E_M{}^V+B_2{}^{\mathrm{I}}}{kT}\right)+16\nu_1C_2{}^{\mathrm{II}}\exp\left(-\frac{E_M{}^V+B_2{}^{\mathrm{II}}}{kT}\right), \quad (44)$$

with

$$C_t=C_1+2(C_2{}^{\mathrm{I}}+C_2{}^{\mathrm{II}}). \quad (30)$$

The fractional concentrations of type-I divacancies $(C_2{}^{\mathrm{I}})_0$ and type-II divacancies $(C_2{}^{\mathrm{II}})_0$ after a quench are given by

$$(C_2{}^{\mathrm{I}})_0=\left\{\frac{[1+8(\xi_{\mathrm{I}}{}^*+\xi_{\mathrm{II}}{}^*)C_t-1]^{1/2}}{4(\xi_{\mathrm{I}}{}^*+\xi_{\mathrm{II}}{}^*)}\right\}^2\xi_{\mathrm{I}}{}^*, \quad (45)$$

$$(C_2{}^{\mathrm{II}})_0=\left\{\frac{[1+8(\xi_{\mathrm{I}}{}^*+\xi_{\mathrm{II}}{}^*)C_t-1]^{1/2}}{4(\xi_{\mathrm{I}}{}^*+\xi_{\mathrm{II}}{}^*)}\right\}^2\xi_{\mathrm{II}}{}^*, \quad (46)$$

where

$$\xi_{\mathrm{I}}{}^*=4\exp(B_2{}^{\mathrm{I}}/kT^*) \quad (47)$$

$$\xi_{\mathrm{II}}{}^*=3\exp(B_2{}^{\mathrm{II}}/kT^*). \quad (48)$$

Using Eq. (30), Eq. (44) can be integrated.

$$C_1=-\frac{1}{16\{\exp(-B_2{}^{\mathrm{I}}/kT)+\frac{3}{4}\exp(B_2{}^{\mathrm{II}}/kT)\}}+\frac{1}{112\nu_1\tau\exp(-E_M{}^V/kT)}\frac{\exp[(t-t_0)/\tau]+1}{\exp[(t-t_0)/\tau]-1}, \quad (49)$$

where

$$\frac{1}{\tau}=\frac{14\nu_1\exp\{-(E_M{}^V+B_2{}^{\mathrm{I}})/kT\}}{1+\frac{3}{4}\exp\{(B_2{}^{\mathrm{II}}-B_2{}^{\mathrm{I}})/kT\}}\left[1+32C_t\left\{\exp\left(\frac{B_2{}^{\mathrm{I}}}{kT}\right)+\frac{3}{4}\exp\left(\frac{B_2{}^{\mathrm{II}}}{kT}\right)\right\}\right]^{1/2}, \quad (50)$$

$$t_0=\tau\ln\frac{16\{\exp(B_2{}^{\mathrm{I}}/kT)+\frac{3}{4}\exp(B_2{}^{\mathrm{II}}/kT)\}(C_1)_0+1-[1+32C_t\{\exp(B_2{}^{\mathrm{I}}/kT)+\frac{3}{4}\exp(B_2{}^{\mathrm{II}}/kT)\}]^{1/2}}{16\{\exp(B_2{}^{\mathrm{I}}/kT)+\frac{3}{4}\exp(B_2{}^{\mathrm{II}}/kT)\}(C_1)_0+1+[1+32C_t\{\exp(B_2{}^{\mathrm{I}}/kT)+\frac{3}{4}\exp(B_2{}^{\mathrm{II}}/kT)\}]^{1/2}}. \quad (51)$$

τ has the dimension of time and is related to how fast the equilibrium divacancies are formed. For iron, $E_M{}^V$ and ν_1 are taken to be 0.9 eV and 10^{13} sec^{-1}, respectively.

Figure 22 shows the plot of the values of τ for the case where $C_t=10^{-5}$. The values of the binding energies of type-I and type-II divacancies are given. If $B_2{}^{\mathrm{II}}$ is

taken to be zero and $\frac{3}{4}\exp(B_2^{II}/kT)$ is ignored, then Eq. (51) becomes Eq. (23) which is the equation for the nearest-neighbor interaction.

VII. CONCLUSIONS AND SUMMARY

Divacancies and trivacancies in body-centered cubic metals have been classified and discussed. For the nearest-neighbor interaction, one type of divacancy and three types of trivacancies are classified. These are 71° trivacancies, 109° trivacancies, and 180°(I) trivacancies. Divacancies have to be broken up into two single vacancies to migrate. For the next-nearest-neighbor interaction there are two kinds of divacancies. Type I has the vacant sites in the nearest-neighbor position and type II has the vacant sites in the next-nearest-neighbor position. There are three more kinds of trivacancies for the next-nearest-neighbor interactions. These are 90° trivacancies, 144° trivacancies, and 180°(II) trivacancies. The general kinetic equations are discussed in detail concerning these defects. The formation of divacancies during quenching and annealing is discussed in great detail. There exists a critical temperature T^* above which the temperature is high enough to maintain thermal equilibrium but below which the motion of single vacancies is too slow to maintain thermal equilibrium in the quenching process. The situation at T^* is frozen in by quenching. After the quench more divacancies are formed and the kinetic equations and the characteristic times for the formation of divacancies are discussed.

ACKNOWLEDGMENTS

The author is grateful for the continuous interest and encouragement of J. S. Koehler and O. C. Simpson. The author is deeply indebted to J. S. Koehler and R. M. J. Cotterill for stimulating discussions. The editorial assistance of D. Larson, R. Flink, and C. Lode is deeply appreciated.

PHYSICAL REVIEW VOLUME 160, NUMBER 3 15 AUGUST 1967

Determination of Anisotropic Momentum Distributions in Positron Annihilation

P. E. MIJNARENDS
Reactor Centrum Nederland, Petten, The Netherlands
(Received 1 March 1967)

A theoretical method is presented which permits the experimental determination of the momentum distribution of the photon pairs originating in positron annihilation in crystalline solids, as a function of both the magnitude and the direction of that momentum. The distribution is expanded in a series of lattice harmonics. It is shown how linear combinations of the two-quantum angular correlations, obtained from measurements on a number of suitably oriented single crystals, may be unfolded to yield the momentum-dependent coefficients in that expansion. The method is illustrated by a model computation.

1. INTRODUCTION

IT is well known that the angular correlation of the annihilation radiation from positrons stopped in oriented single crystals[1–5] may provide information on the electronic structure of the substance under study and, in metals, on the shape of the Fermi surface. The intensity of the two-quantum angular correlation $N(p_z)$, measured with the long horizontal slit apparatus commonly used,[2] is proportional to the probability that the photon pair carries off a momentum with a component along the z axis of the instrument between p_z and p_z+dp_z. This probability is related to the probability that the pair of annihilation quanta has a total momentum $\mathbf{p}$, i.e., the photon-pair momentum distribution $\rho(\mathbf{p})$, by

$$N(p_z) \propto \int_{-\infty}^{\infty}\int_{-\infty}^{\infty} \rho(\mathbf{p})dp_x dp_y. \quad (1)$$

In general, $\rho(\mathbf{p})$ is anisotropic owing to the presence of the lattice potential,[2] while it is also influenced by many-body effects like electron-electron and electron-positron correlations.[6,7] The detailed behavior of $\rho(\mathbf{p})$ will therefore yield information concerning those effects.

The extraction of this information from the experimental data is complicated by the fact that one does not directly measure $\rho(\mathbf{p})$ but rather its integrals over slices of momentum space characterized by certain values and orientations of p_z, as expressed by Eq. (1). Of

[1] S. Berko, R. E. Kelley, and J. S. Plaskett, Phys. Rev. **106**, 824 (1957).
[2] S. Berko and J. S. Plaskett, Phys. Rev. **112**, 1877 (1958).
[3] A. T. Stewart, J. B. Shand, J. J. Donaghy, and J. H. Kusmiss, Phys. Rev. **128**, 118 (1962).
[4] J. J. Donaghy, A. T. Stewart, D. M. Rockmore, and J. H. Kusmiss, in: *Proceedings of the IXth International Conference on Low Temperature Physics, Columbus, Ohio*, edited by J. G. Daunt, D. O. Edwards, F. J. Milford, and M. Yaqub (Plenum Press, Inc., New York, 1965), Part B, p. 835.
[5] B. Rozenfeld, W. Swiatkowski, and J. Wesolowski, Acta Phys. Pol. **29**, 429 (1966).
[6] S. Kahana, Phys. Rev. **117**, 123 (1960); **129**, 1622 (1963).
[7] C. K. Majumdar, Phys. Rev. **140**, A227 (1965); **140**, A237 (1965).